Int J Earth Sci (Geol Rundsch) (2005) 94: 66–93
DOI 10.1007/s00531-004-0446-z

ORIGINAL PAPER

Thore Szeder · Frank Sirocko

Evidence for active tilting of the NW-German Basin from correlations between fluvial landscape and geological subground

Received: 12 November 2003 / Accepted: 16 September 2004 / Published online: 27 January 2005

Abstract The catchment basin of the River Hunte (Lower Saxony, NW-German Basin) was studied on a mesoscale (length of ~90 km) to investigate the influence of the geological subground on modern morphology. A Geo Information System (GIS) was used to calculate linear correlation coefficients between the depth of geological strata (Base Zechstein to Base Quaternary) and the height of the modern landscape (Holocene Alluvial Plain, Lower Weichselian Terrace, catchment basin and watershed). High linear correlation coefficients between the Base of Tertiary and the height of the modern topography (catchment basin [$r^2 = 0.87$], Lower Weichselian Terrace [$r^2 = 0.95$] and Holocene Alluvial Plain [$r^2 = 0.95$]) indicate control of the modern topography by the depth of the geological subsurface via tilting of the entire basin. Most likely northward tilting of the NW-German Basin forces the River Hunte to flow in a northerly direction by relative uplift of the hinterland (Wiehengebirge, Rhenish Massif) and subsidence of the North Sea area.

Keywords North-German Basin · Active tectonics · Rivers · Surface morphology · GIS

Introduction

Geographical position of the study area

Figure 1 shows the geographical position of the study area (black rectangle). The investigated part of the River Hunte catchment basin is given in yellow. The River Hunte is the northerly left positioned tributary of the River Weser. The area of the total catchment basin is about 2,640 km^2. The well is on the southern slope of the German Middle Mountain range (“Wiehengebirge”) at 150 m a.s.l..

The River Hunte reaches the North German plain after a distance of ~8 km, at a height of about 50 m a.s.l.. After a distance of 37 km, the river reaches the Lake Dümmer. Near the town Barnstorf (Fig. 2), the River Hunte enters the hilly and undulating area of the “Cloppenburger and Wildeshauser Geest”, formed by the glacial deposits of the Saalian glaciation. North of the town Oldenburg, the River Hunte reaches the marshy area of the River Weser. Here, the river is already under tidal influences of the North Sea. The Hunte flows into the river Weser after a total length of ~110 km near the town Bremen at a height of about 0 m a.s.l. (Ness 1994).

Structural and geological situation of the study area

The study area is positioned in the NW-German Basin. The NW-German Basin is part of the Central European Basin, which extends from the North Sea through NW-Germany to the Polish lowland. The evolution of the basin must be seen in the context of the tectonic evolution of Europe (Ziegler 1990). Multiple deformation phases occurred since the initial basin formation in the Early Permian around 290 Ma ago with continuous and sometimes rapid change in stress regime. Basement faults, already initiated during the pre-Permian Variscan Orogenese, became reactivated during later rifting and inversial times. The NW-German Basin was completely reorganised structurally during the Upper Cretaceous inversion. The tectonic evolution (stress regime) triggered the basin geometry and therefore the distribution of sediments (Ziegler et al. 1995). Even the distribution and orientation of salt structures is connected with deep fault zones/lineaments of the deeper crust (Baldschuhn et al. 2001). Intensive exploration of the Oil Industry over the last decades led to a dense net of drillings and seismic data. Most of the structural and geological

T. Szeder (✉) · F. Sirocko
Institute for Geoscience,
Johannes Gutenberg-Universität Mainz,
55099 Mainz, Germany
Tel.: +49-6136-925376
E-mail: thore_szeder@web.de

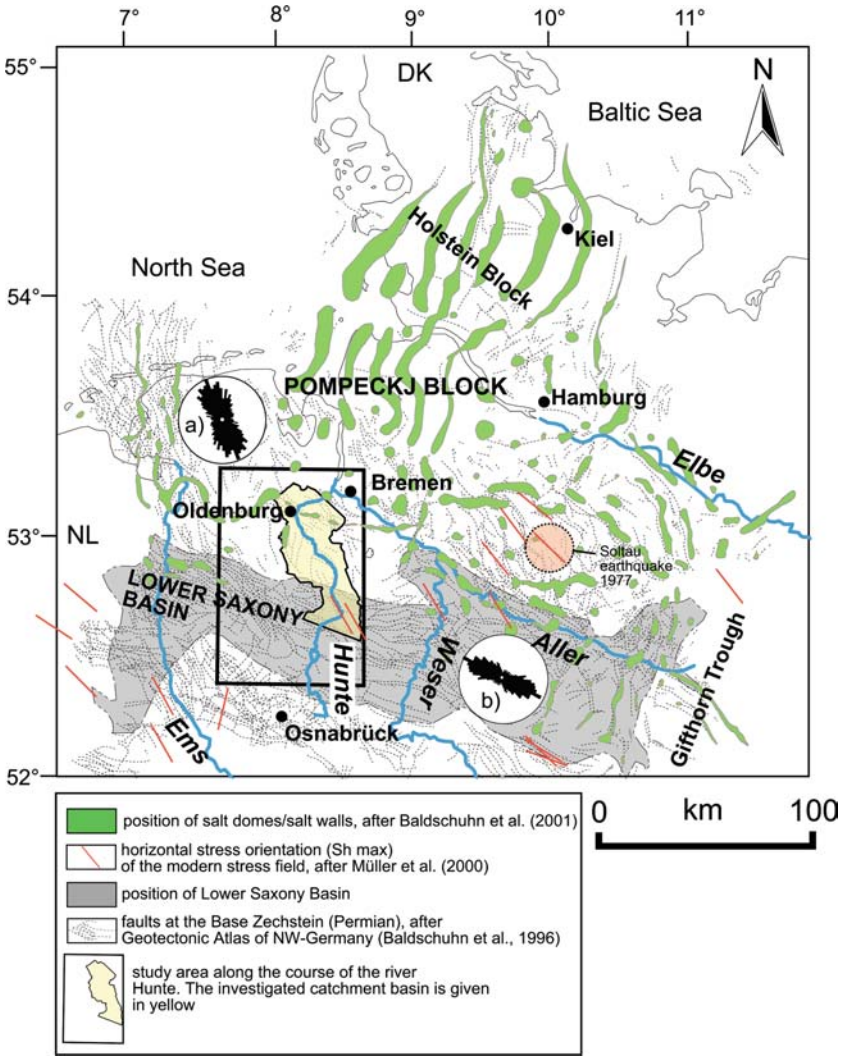

Fig. 1 Structural situation of the NW-German Basin. The position of salt domes and salt walls is given in *green* (after Boigk 1981). The faults at the Base Zechstein (Permian) are shown in *black* (*dashed lines*), (after Baldschuhn et al. 1996). The position of the Lower Saxony Basin is presented in *gray*, (after Boigk 1981; Betz et al. 1987). The position of modern horizontal stress orientation measurements (Sh max) are presented in *red lines*, after World Stress Map Data Base (Müller et al. 2000). The position of the Soltau, 1977 tectonic earthquake with the orientation of the striking fault plane (*red line*) is marked by the *red circle*, (after Leydecker et al. 1980). The rose diagrams show the orientation of the faults at the Base of Zechstein for **a** the Pompeckj Block and **b** the Lower Saxony Basin, plotted by length with a pedal width of 5°

knowledge on the NW-German Basin is based on this data (Boigk 1981).

Figure 1 shows the position of the study area (black rectangle) in relation to the main structural units of the NW-German Basin. The southernmost part of the investigated part of the River Hunte catchment basin (yellow field) is located above the Lower Saxony Basin (gray field) and most of the northern area is located above the northerly adjacent tectonically more stable Pompeckj block. The black dashed lines mark the faults at the Base of Zechstein after the Geotectonic Atlas of NW-Germany (Baldschuhn et al. 1996) and the green areas the position of salt domes and salt walls after (Boigk 1981). The rose diagrams show the strike direction for the faults at the Base of Zechstein for (a) the Pompeckj Block and (b) for the Lower Saxony Basin. The geographical orientation of the Lower Saxony Basin is WNW. This direction is also shown by the orientation of the faults at the Base of Zechstein. Most of the Zechstein faults on the Pompeckj Block are striking with NNW (Fig. 1a). Salt walls and a salt dome can be found only in the northernmost part of the study area.

The basement of the NW-German-Basin is separated into numerous basementblocks. Fig. 3 shows this pattern for the study area (Baldschuhn et al. 2001). The red lines give the position of lineaments and faults at the basal Zechstein or below, which separate the basement blocks. The faults at the Base of Zechstein are given in black dashed lines after the Geotectonic Atlas of NW-Germany (Baldschuhn et al. 1996). The gray circled letters A to I give the names of basement blocks, and the watershed of the River Hunte is shown in black. Rivers are given in blue, and the Holocene Alluvial Plain of the River Hunte in yellow. The Goldenstedt Blenhorst Lineament (number 3) in the east and the Rheder Moor Oythe Lineament (number 4) in the west separate the Lower Saxony Basin in the south from the Pompeckj Block in the north. The basement block E (Bockstedt Graben Lessen-Staffhorst-Block) is the northernmost block of the study area between the Lower Saxony Basin and the Pompeckj Block. It is part of a 70–80 km extending NNE vergent overthrust block (Baldschuhn et al. 2001). The Leer-Bremen-Lineament (number 1) which can be found on the Pompeckj Block separates the

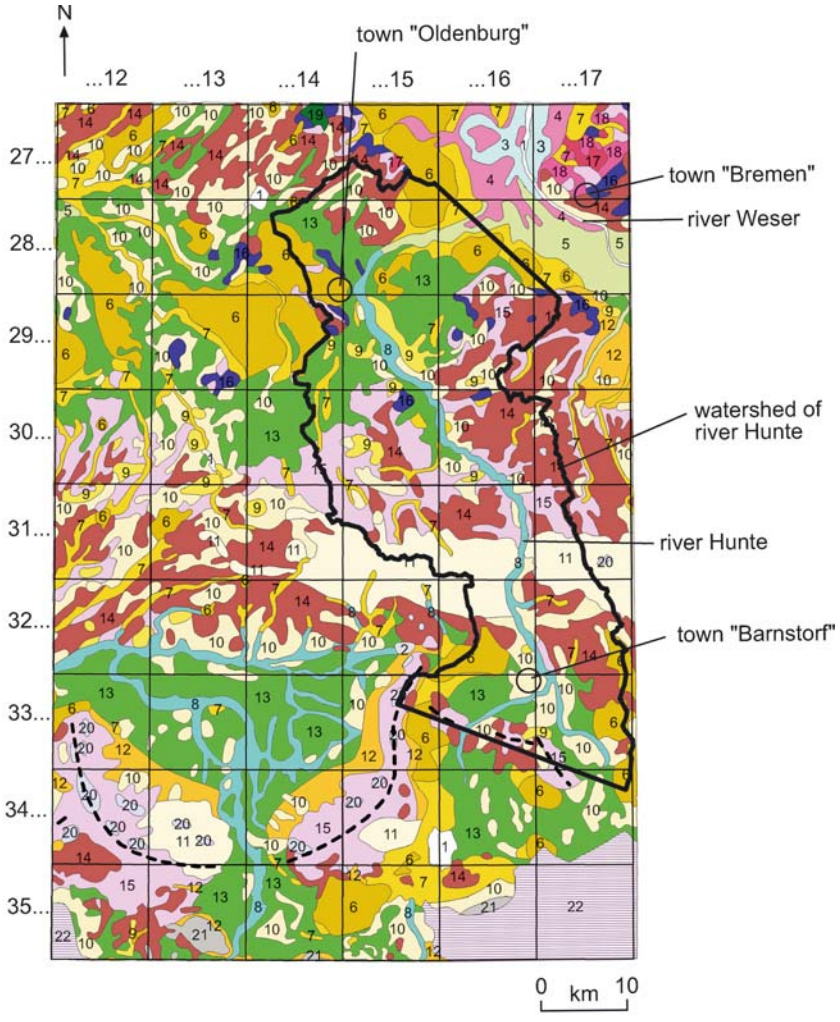

Fig. 2 Geological map; the grid shows the name (numbers) and position of the topographic maps. The black field shows the investigated part of the River Hunte catchment basin. **Holocene** *1* water, *2* anthropogenic replenishment, *3* mudflat deposits, *4* brackish water deposits, *5* tidal deposits, *6* highmoor deposits, *7* lowmoor deposits, *8* alluvial-plain deposits, *9* dune sands; **Pleistocene** *Weichselian 10* cover sands, *11* sandy loess, *12* sediments of solifluction, *13* lower terrace, *Saalian 14* morainic deposits, *15* meltwater sands, push-end-morain (*dashed line*), *Elsterian 16* deposits of glacial meal ''Lauenburger Ton'', *17* morainic deposits, *18* meltwater sands, *Pre-Elsterian 19* fluvial deposits of the oldest terraces, **Pre-Quaternary:** *20* Tertiary (transported by glacials), *21* mesocoic sediments, *22* unmapped area. (After NLfB 1993)

Ostfriesland Block in the north (A, B) from the Südoldenburg Block in the south (C, D). The NNW orientated Berdum-Jaderberg-Sagermeer-Fault (number 2) partitions the Ostfriesland Block into the westward Ostfriesland West-Block (A) and the eastward Ostfriesland East Block (B) and the Südoldenburg Block into the Südoldenburg Block West (C) and the Südoldenburg Block East (D).

In the following sections, important structural elements of the study area, which were crossed by the River Hunte, will be explained. Figure 4 shows the structural situation at the Base of Upper Cretaceous with the position of structural elements. The depth is given from white (−100) to black (−3,300 m a.s.l.). The faults are shown in red, salt structures (salt domes and salt pillows [dashed line] in blue) and outcrop of the Upper Cretaceous are shown in pink. The position of the investigated section of the River Hunte catchment basin is given in yellow and the Holocene Alluvial Plain of the River Hunte in green.

The structure ''Oldenburg-Delmenhorst'' is an inverted graben (bipolar inversion structure) modified by injection of salt. Like the structure ''Zwischenahn'' it is part of the Leer-Bremen-Lineament (Fig. 3, number 1). A graben structure was formed due to movements at the basement during the Middle Jurassic, and Zechstein salts rose up. During the inversional phase in the Upper Cretaceous (Coniac-Santon), the graben fill was squeezed on the former graben shoulder. This bulge process lasted until the Younger Tertiary as documented by outcrops on top of the structure. Due to this bulging and stretching during the Tertiary, a graben was formed on top (Fig. 5). It is remarkable that in the deeper geological strata the single structural elements are in accordance with the basement pattern. Firstly, in the Tertiary the structural connection between ''Oldenburg-Delmenhorst'' and ''Zwischenahn'' was formed by keystone faulting (Fig. 5), (Baldschuhn et al. 2001).

Doming of the geological depth above the salt pillow ''Dötlingen'' is visible from the Base of Lower and Middle Buntsandstein to the Base Middle Oligocene to Upper Oligocene (Baldschuhn et al. 2001). The graben structures ''Goldenstedt, Norddöllen, Bockstedt'' are part of the Bockstedt Graben Lessen-Staffhorst-Block (Fig. 3, letter E). These Graben structures formed during Triassic to Jurassic times. During the inversional

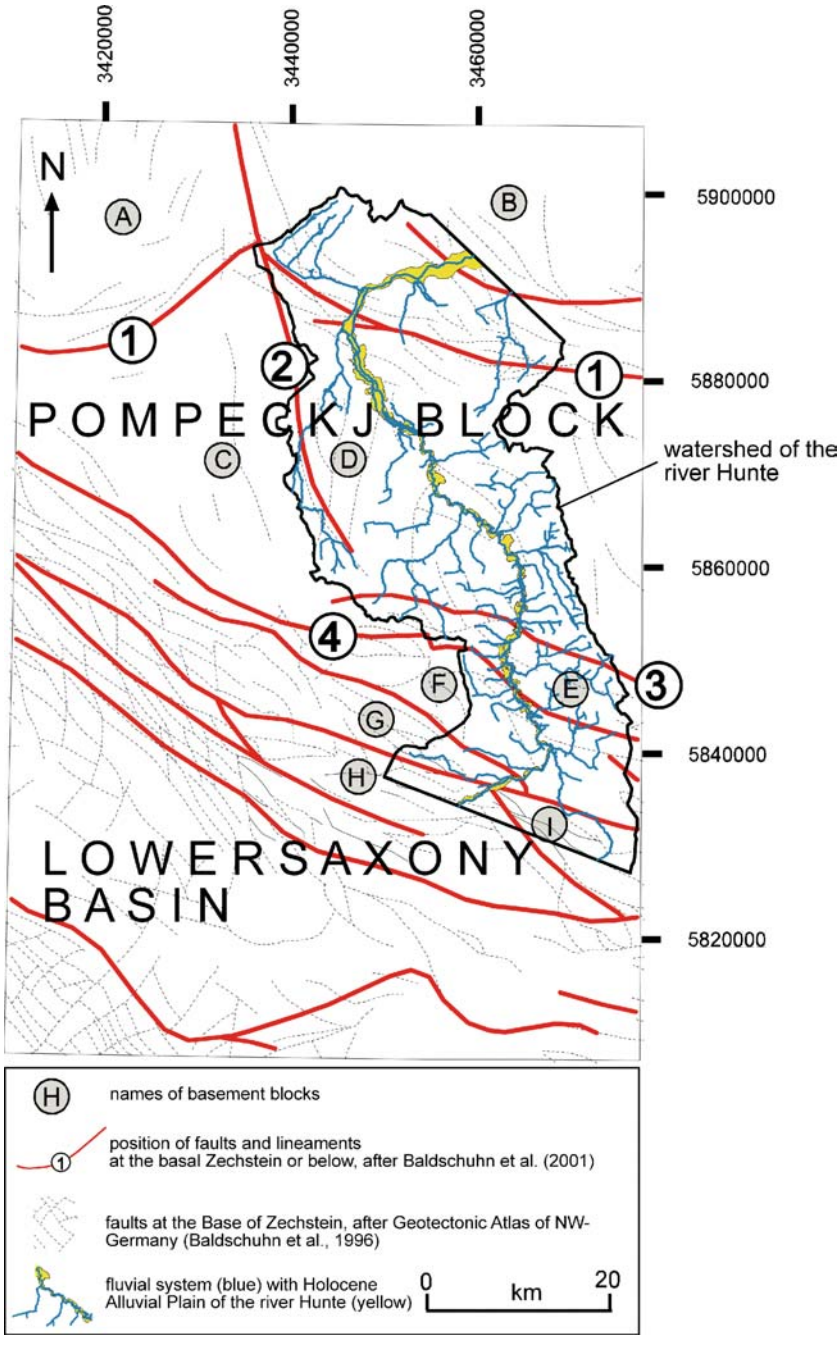

Fig. 3 Structural situation (pattern of basement blocks) of the study area (after Baldschuhn et al. 2001). The *red lines* show the position of faults, structure zones and lineaments at the basal Zechstein or below. *1* "Leer-Bremen-Lineament", *2* "Berdum-Jaderberg-Sagermeer-Fault", *3* "Goldenstedt Blenhorst Lineament" and *4* "Rheder Moor Oythe Lineament". The *gray circled letters (A–I)* stand for the names of basement blocks. The blocks *A–D* are positioned on the Pompeckj Block, *E–I* on the Lower Saxony Basin. *A* Ostfriesland West-Block, *B* Ostfriesland East-Block, *C* Südoldenburg Block West, *D* Südoldenburg Block East, *E* Bockstedt Graben Lessen-Staffhorst-Block, *F* Oythe-Düste-Wehrbleck-Block, *G* Dersum-Börger-Hemmelte-Bokern-Block, *H* Kroge-Diepholz-Neufeld-Block, *I* Rheden-Bahrenborstel-Block. The *dashed black lines* show the faults at the Base of Zechstein after the Geotectonic Atlas of NW-Germany (Baldschuhn et al. 1996). The position of the investigated part of the River Hunte watershed is given by the *bold black line*, rivers are shown in *blue* and the Holocene Alluvial Plain of the River Hunte in *yellow*

phase of the Upper Cretaceous (Coniac-Santon) the graben structures were uplifted and the former peripheral faults transformed to gently dipping NE-vergent thrust zones. At this inversional phase, Zechstein salt penetrated into the overthrust sheets (Triassic, Bundsandstein, Röt) and formed salt wedges. The salt wedges amplified the process of anticlinal formation (Baldschuhn et al. 2001).

The inversional, anticlinal structure "Aldorf" is positioned on the Oythe-Düste-Wehrbleck-Block (Fig. 3, letter F). The W-E striking anticlinal structure is visible from the Base Upper Buntsandstein and Muschelkalk to the Base of Tertiary (Baldschuhn et al. 2001). The weak inversion (during Upper Cretaceous [Coniac/Santon]) of the structure was founded by the thrusting of the basement and the Triassic strata and the intrusion of Zechstein salts into the Upper Buntsandstein (Rötsalinar) and the linked doming of the overlying strata (Baldschuhn et al. 2001). The counterpart of these anticline structures like "Aldorf" is the formation of marginal troughs like the Upper Cretaceous trough "Donstorf".

Development of salt structures

Most of the NW-German salt structures were already developed during the Lower Triassic as salt pillows. The diapiric stage was reached by most of them during the

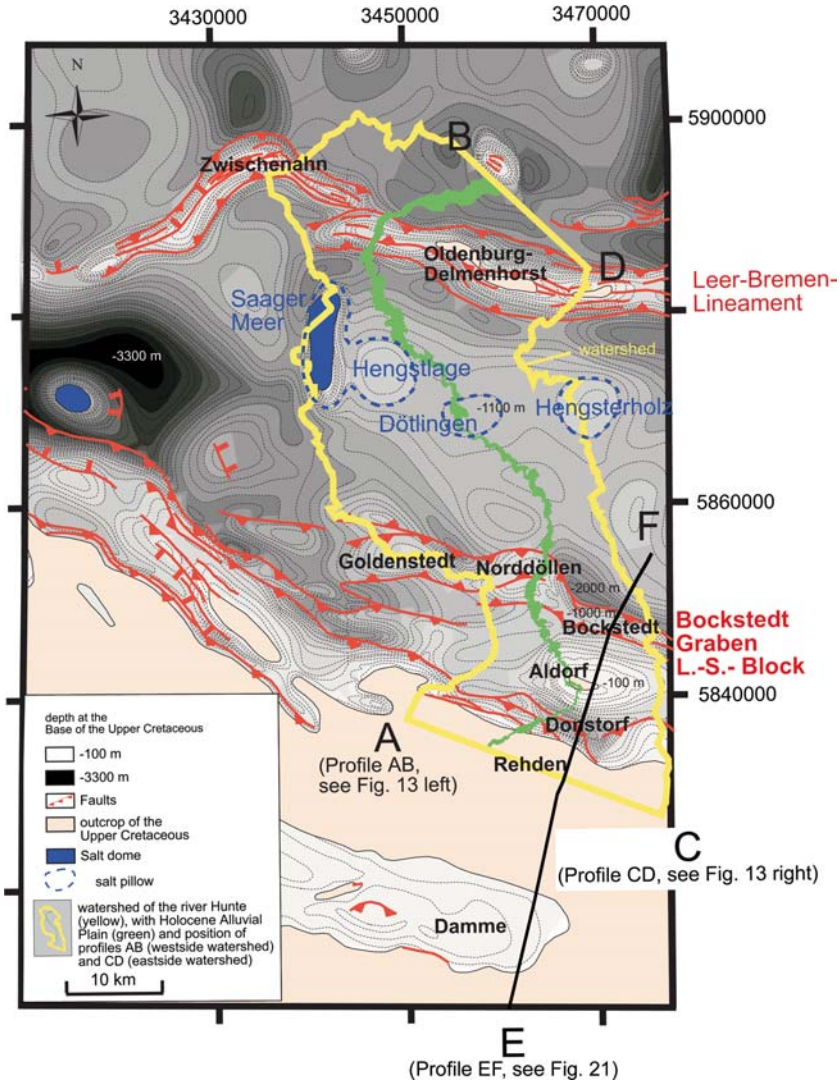

Fig. 4 Section of the River Hunte catchment basin with position of the watershed (*yellow*), Holocene Alluvial plain (*green*), depth at the Base of Upper Cretaceous from −100 (*white*) to −3300 m (*black*), faults (*red*), outcrop (*pink*), salt domes (*blue*), salt pillows (*dashed blue*), with structural names of tectonic blocks, salt structures and major lineaments, (after Baldschuhn et al. 2001; Baldschuhn et al. 1996). Position of profile AB (westerly watershed) is shown in Fig. 13, left, profile CD (easterly watershed) in Fig. 13, right, and profile EF in Fig. 21

Upper Triassic (Keuper), (Jaritz 1992). The difference in the structural development of the Lower Saxony Basin and the tectonically more stable Pompeckj Block is also reflected in the development of the salt structures. Whilst the climax of diapirism on the Pompeckj Block occured during the Triassic, the phase of diapirism in the Lower Saxony Basin was linked to the inversional phase during the Upper Cretaceous (Jaritz 1973). The genesis of the Lower Saxonian Tectogene led to the formation of salt wedges. Permian salts intruded and filled extensional joints of the overlying strata during the pre-Upper Cretaceous tensional rifting phases. During the compressive phase of basin inversion, these salts were pressed into the adjacent strata, diapirs and salt pillows were squashed and transformed and pre-Permian basement blocks were uplifted (Baldschuhn et al. 1998).

The average uplift rate of the NW-German salt domes in the diapiric stage varied between 0.1 and 0.5 mm/a, and in the later stages only several hundredths of a millimetre were reached (Jaritz 1980). After Jaritz (1992) about two-thirds of the three hundred NW-German salt structures were induced by tectonics and numerous diapirs were affected in their structural evolution by tectonism.

Orientation of the modern stress field and seismicity

The red lines in Fig. 1 show the orientation of strain measurements (Sh max) after the World Stress Map (Müller et al. 2000). Two measurements were available from the southern part of the study area, showing a stress orientation of 150°. Nearly the same orientation can be found westerly of the study area between the River Weser and Elbe.

Northern Germany is an area of low seismicity (Leydecker 2002b; Leydecker and Kopera 1999). A historical earthquake occurred in AD 1770 about 25 km north of Osnabrück at the southern margin of the Lower Saxony Basin, probably the strongest earthquake in Northern Germany over the last 1,000 years (Leydecker et al. 1980). Since the times of instrumental earthquake recording, two tectonic earthquakes have been detected for Northern Germany. The first in the year 1977 near the town Soltau about 50 km south of Hamburg

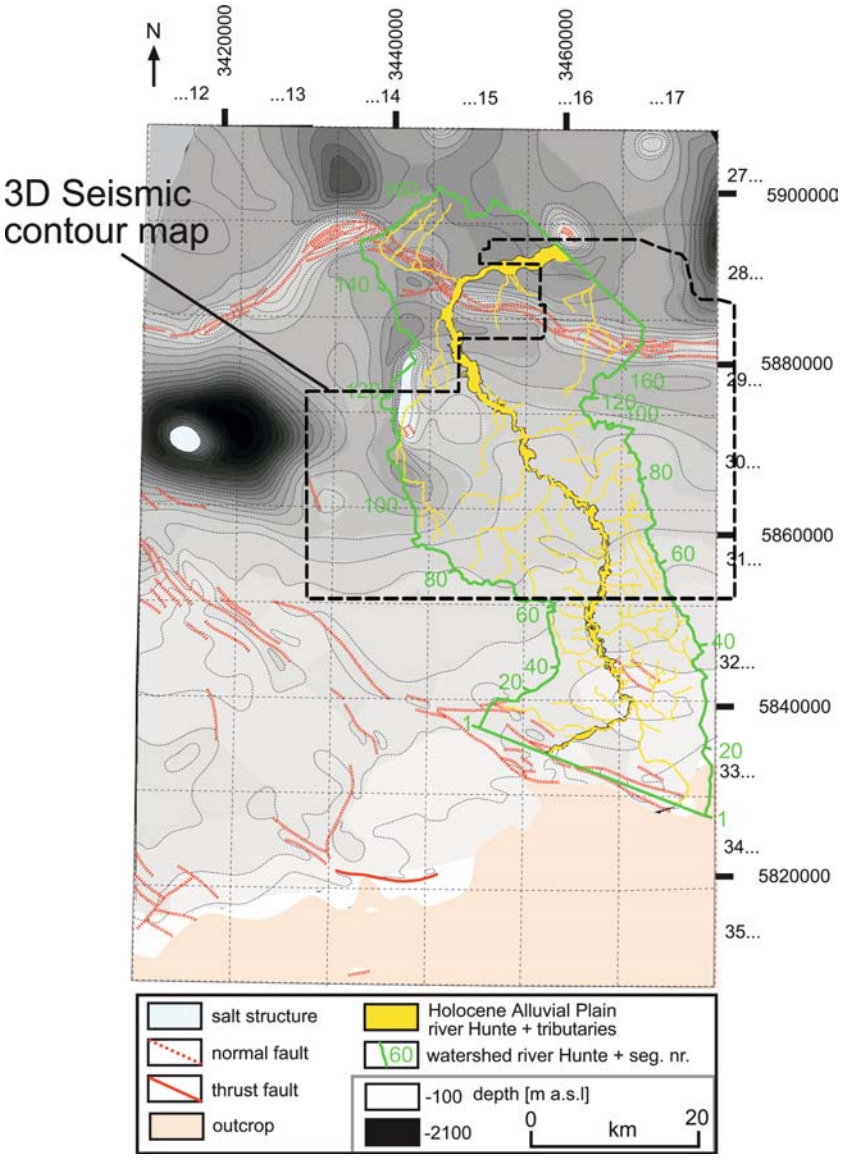

Fig. 5 Structural geological situation of the study area at the Base of Tertiary. The position of salt walls and salt domes is given in *blue*, thrust faults (*red*) and normal faults (*red with a dashed line*), outcrop (*pink*), the depth is given from *white* (highest position) to *black* (lowest position), after Geotectonic Atlas of NW-Germany (Baldschuhn et al. 1996). The Holocene Alluvial Plain of the River Hunte and tributaries (*yellow*), watershed of the River Hunte (*green*) with the position of the segment lines, after topographical maps (LGN 1898; LGN 1994). The *dashed squares* show the position of the topographical maps with map number

(9°56.7E + −9.0 km; 52°56.9N + −5.5 km) with a magnitude of ML = 4.0. The focal depth was between 4 and 13 km, probably near the bottom of the Zechstein or pre-Zechstein sequence. A NNW-SSE striking fault plane is favoured because of local geological conditions (Leydecker et al. 1980), (Fig. 1, red circle). The second one occurred in the year 2000 at Zarrentin/Wittenburg 20 km SW of Schwerin near the river Elbe with a magnitude of ML = 3.2 (Leydecker 2002a).

Upper cretaceous (sub-hercynian phase)

The convergence of Africa/Arabia with Eurasia finally resulted in the collision of the Alpine orogen with the southern passive margin of Europe. Collisional coupling of the Alpine orogen with its foreland is thought to be responsible for the onset of intra-plate compressional deformation of Western and Central Europe (Ziegler et al. 1995; Ziegler 1990). This Senonium Sub-Hercynian phase of compression led to the inversion of the Lower Saxony Basin. The Lower Saxony Basin was transformed to the Lower Saxony Tectogene by this process. Faults became reactivated and sediment fill was thrust over the northerly adjacent stable Pompeckj Block. Faults at the Base of Zechstein became reversed at this time. This inversion tectonism led to a substantial uplift of the pre-Permian layers (Betz et al. 1987). Late Permian salts served as detachment planes (Baldschuhn et al. 2001). While the Lower Saxony Block was uplifted, the northerly Pompeckj Block subsided. This led to accumulation of up to 2,000 m of sediments (marlstones, light chalkstones [“Schreibkreide”]) in the area of the Pompeckj Block. Inversion structures are not only restricted to the Lower Saxony Basin, they can also be found on the Pompeckj Block. Most of the inversion structures are coupled to basement faults. During the phase of inversion (Coniacian–Campanian) the sedimentary fill of the grabens was thrust over the graben

shoulders. Salt domes were tectonically superimposed and subsequent movements of halocinetic structures led to local variation of thickness, hiatus and facies changes (Baldschuhn et al. 1985; Boigk 1968).

Tertiary (65.5–1.8 Ma)

During the Upper Paleocene, a first transgression of the Tertiary shallow epicontinental sea reached the south of Lower Saxony (Hinsch and Ortlam, 1974). During the Eocene, the sea expanded again and reached its greatest size in the Oligocene. A connection from the North Sea via the Hessian Depression to the Mainz Basin and the Rhenish Graben existed during the Middle Oligocene (Gramann 1966). During the Upper Oligocene, the sea regressed and the connection to the Mainz Basin closed up. Isolated transgression phases with permanently changing shallow sea, and brackish to terrestrial conditions occurred during the Miocene, when flat islands or depressions were formed by salt domes. In the Pliocene, the sea retreated to the westerly part of Schleswig-Holstein and the Ems estuary. Limnic and fluviatile sediments were deposited. The sediment thickness of the Tertiary sediments varies strongly, because it is influenced by halocinetic processes. In the rim synclines of the salt structures, more than 3,000 m of Tertiary sediments were deposited locally.

During the mid-Paleocene, a second phase of basin inversion occurred (Laramide-phase), which is evident in the Lower Saxony Basin, the West Netherland Basin and the Central Graben of the North Sea (Betz et al. 1987). The most distal inversion structures can be observed in the Central North Sea, which is about 1,400 km far from the Alpine thrust front. The compressional deformation was interrupted at the end of the Paleocene but resumed during the late Eocene and Early Oligocene. The evolution of the European Cenozoic rift system at Eocene and younger times is mostly synchronous with the compressional intra-plate deformations of the nortwestern Alpine foreland. These rift systems, which can be traced from the western Mediterranean to the coastal area of the North Sea, became evidental during the Middle Eocene to Early Oligocene (Ziegler et al. 1995). The last inversion moments in the Lower Saxony Basin could be observed in the Early Oligocene. The Lower Saxony Basin was smoothly uplifted during the Mio-Pliocene. This trend is coupled with the thermal doming of the Rhenish Massif, which was related to the evolution of the Rhine Graben System (Betz et al. 1987). Contemporaneously, the Leine Graben was uplifted. The present day stress field was established during the Mio-Pliocene transition, which is characterised by NW directed trajectories of maximum horizontal compression (Müller et al. 1992). Broad scale negative deflection of the North-Sea basin lithosphere is indicated by Plio-Pleistocene subsidence rates (Cloetingh et al. 1990; Cloetingh and Kooi 1992; Ziegler et al. 1995; Ziegler 1990).

Quaternary development of the study area (1.8–0 Ma)

The area of Lower Saxony was reached for the first time by Scandinavian inland glaciers during the Elsterian. In some cases, the glacials possibly overstepped the border of the German Middle Mountains (Kaltwang, 1992). A net of Elsterian glacial tunnel valleys is detectable from Poland to the Netherlands (Schwab 1996). These channels cut up to 500 m into the ground by hydrostatic pressure, which was built up by the overlying glaciers and eroded the pre-Quaternary strata strongly (Kuster and Meyer 1979; Ortlam and Vierhuff 1978). The Saalian Glacial deposits form most of the modern Lower Saxony topography. The oscillating ice margins formed high push-end moraine walls of up to 150 m (e.g. "Dammer Berge"). The push-end moraine wall of the Rehburger Phase can be traced between Hannover and the Netherlands.

The Scandinavian inland glaciers did not pass the river Elbe during the Weichselian (115–10 ka BP). Consequently, Lower Saxony was under periglacial permafrost conditions (Böse 1995; Liedtke 1981; Mol et al. 2000; Vaikmäe et al. 1995; Vandenberghe 1993; Vandenberghe and Pissart 1993). Aeolian transported sandy loess and coversands can be found there (Meier 1996; Pyritz 1972; Schwan 1988; Vierhuff 1967). The spare vegetation and the thaw of the active permafrost layer led to solifluction processes (Caspers and Freund 2001; Caspers et al. 1995). The river valleys were filled with sandy deposits ("Talsande") from the adjacent higher areas and the Lower Weichselian Terrace was aggregated (Vandenberghe 1992b).

The Late Glacial (13–10 ka BP) marks a transitional time for the NW-European rivers from a braided to meandering pattern due to the change in climate and associated change in vegetation. The rivers started to incise into the previously deposited Lower Weichselian Terrace and by this process formed the Holocene Alluvial Plain (Huisink 1998; Vandenberghe 1993; Vandenberghe 1995a; Vandenberghe 1995b; Vandenberghe et al. 1994).

Figure 2 shows the geological map of the study area after the Quaternary Overview Map of Lower Saxony and Bremen (NLfB 1993). The grid gives the numbers and positions of the topographical maps. The small numbers (1–21) present the lithological units of the Holocene (1–9), the Pleistocene (10–19) with the Weichselian (10–13), the Saalian (14–15), the Elsterian (16–18) and pre-Elsterian (19) and the pre-Quaternary (20–21). The investigated part of the River Hunte catchment basin is shown in black.

It is evident that the study area is dominated by Saalian deposits (meltwatersands [15] and morainic deposits [14]). The glacial Saalian deposits have been the sediment source for the geologically younger Lower Weichselian Terrace [13]. An E-W striking sandy loess cover [11] is visible at the River Hunte catchment basin. This aeolian coversand is disconnected by the ~NS striking River Hunte. The geological map 1:200.000

(BGR 1982) shows that this sandy loess superimposes Saalian morainic deposits. The River Hunte breaks through the higher elevated Saalian deposits (called "Geest") in the south above the anticline structure "Aldorf" and leaves it above the saltpillow "Hengstlage" (Fig. 4). The Digital Elevation Model of the River Hunte catchment basin (Fig. 6) illustrates this breakthrough of the River Hunte. South and north of the "Geest", a wider Lower Weichselian Terrace than inside the "Geest" area is visible (Fig. 7).

Material and methods

Figure 8 shows the principal steps (A to F) which were applied to correlate the height of the modern landscape with the depth of the geological subsurface.

Software and maps

Software

The program Erdas Imagine 8.5 was used for the process of georeferencing. Redrawn and digitised maps were transformed into an orthogonal coordinate system (German National System, Gauss Krueger, system of ninth longitude), (Fig. 8, steps A and B). Map informations were vectorised from the georeferenced maps with the program ArcView GIS 3.2, (Fig. 8, step C). The program was used for the construction of Digital Spatial and Digital Elevation Models (Fig. 8 steps D2 and D3), spatial data requests (Fig. 8, step E) and the final map production (graphical presentation of results). The programs Excel and Microcal

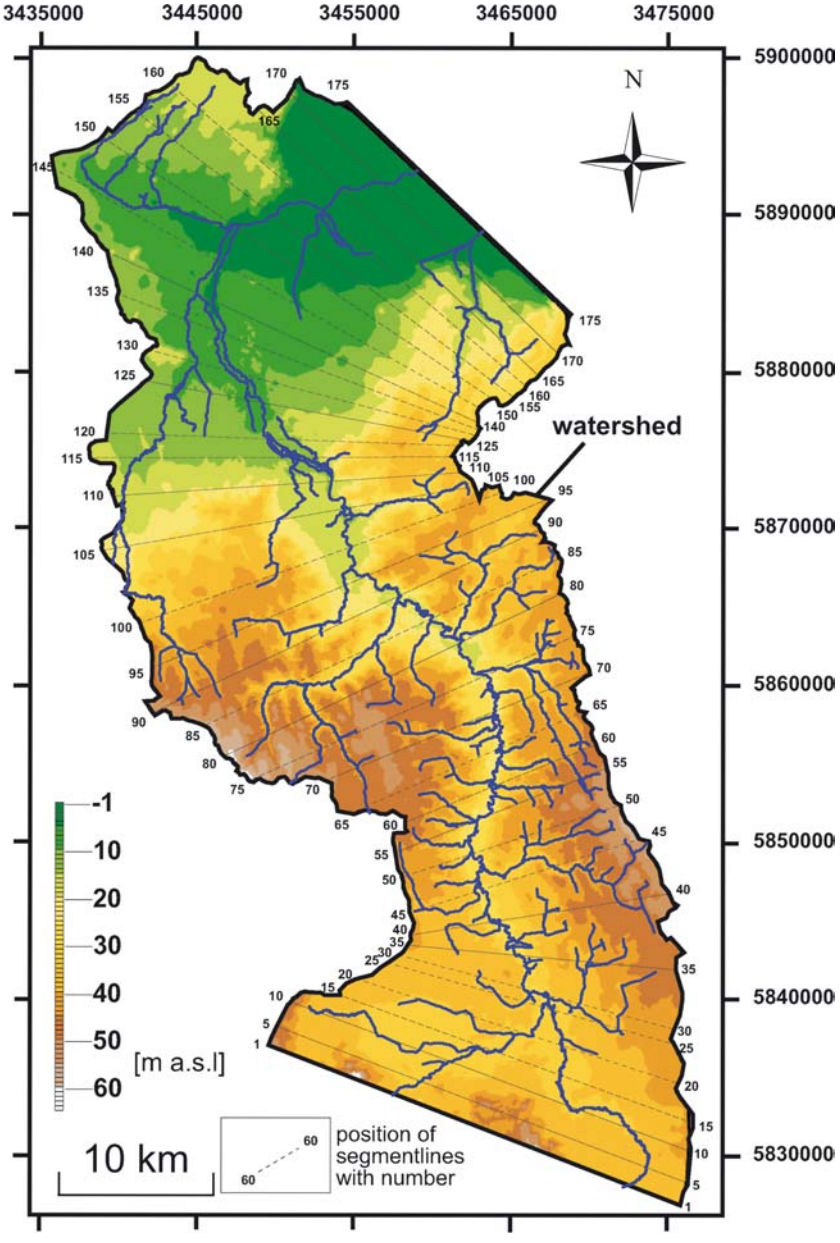

Fig. 6 Digital Elevation Model (DEM) for a section of the River Hunte catchment basin. Range of altitude is +65.0 to −0.69 m a.s.l.. Database: Topographical Maps (LGN 1898; LGN 1994). The *numbered dashed lines* give the position of segment lines. The fluvial system is shown in *blue*

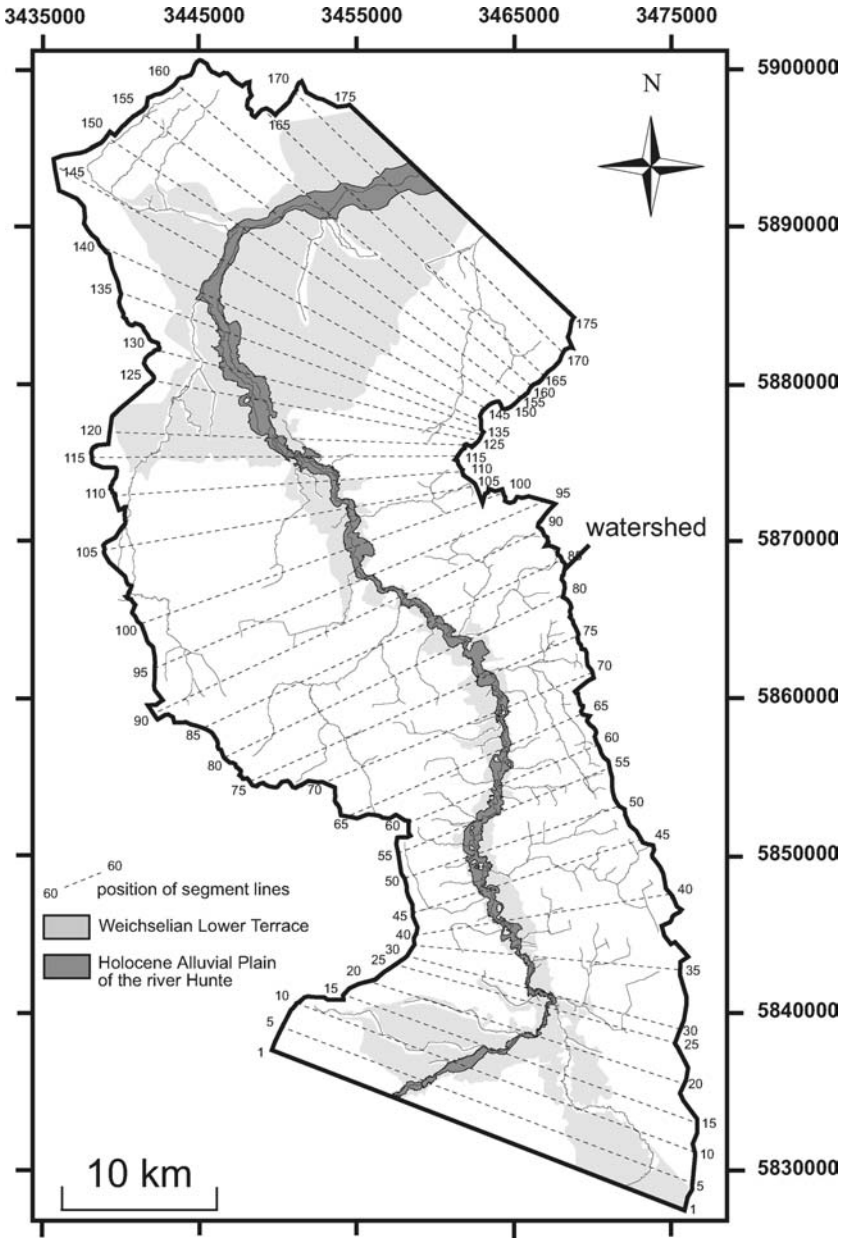

Fig. 7 Section of the River Hunte catchment basin with position of the Holocene Alluvial Plain, Weichselian Lower Terrace, tributaries (with identification number), watershed and segment lines with identification numbers. Holocene Alluvial Plain and the Lower Weichselian Terrace after field work, topographical- and geological maps (BGR 1982; LGN 1898; LGN 1994). The fluvial system is based on the historical topographical maps and the position of the watershed on the modern and historical topographical maps (LGN 1898; LGN 1994)

Origin 6.0 were used for the production of plots and for statistics (calculation of linear correlation coefficients), (Fig. 8, steps F1 and F2).

Topographical maps

A total of 26 historical topographic maps (LGN 1898) and 26 modern topographical maps (LGN 1994) were used for geomorphological analyses. The position of the used maps is given in Fig. 5. The historical maps were used because the courses of the rivers were straightened, and natural slopes and depressions were smoothed due to land-clearance projects about 40 years ago (Ness 1994). The topographical maps (historical and modern) have a contour interval of 1.25 m.

Geological maps

Geological Maps on the scale 1:200,000 (CC3910, CC3110), (BGR 1982) were used to support the mapping of the Holocene Alluvial Plain and the Lower Weichselian Terrace. The Geological Map (NLfB 1993), was used for the presentation of the Quaternary-Geological situation of the study area (Fig. 2).

Structural geological maps

Structural-geological informations about the subsurface were taken from the Geotectonic Atlas of NW-Germany. This atlas was recently published as a paper

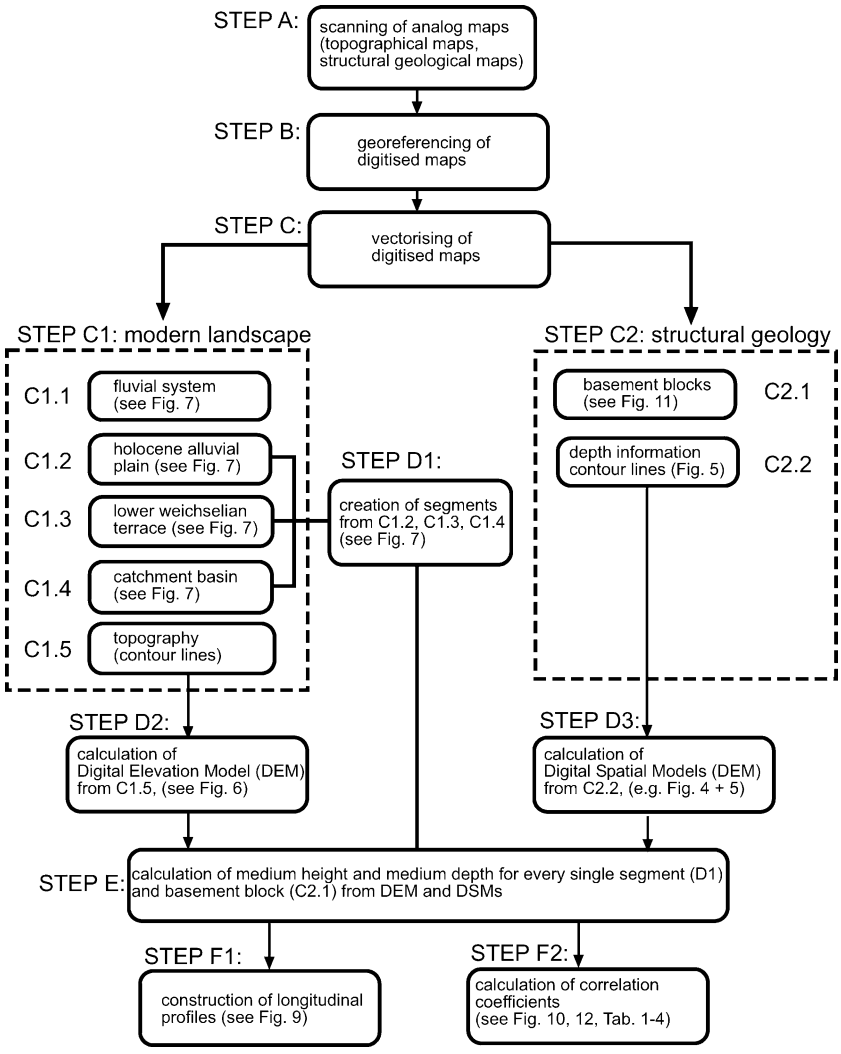

Fig. 8 Principal steps (*A–F*) in the procedure of correlating the height of the modern landscape with the depth of the geological subsurface

map (Baldschuhn et al. 1996) and in electronical mode on CD (Baldschuhn et al. 2001). It gives a synthesis of geological and geophysical data (from about 75,000 deep wells and about 1,000,000 km of reflection seismic lines) made available from the German oil industry. Structural contour maps of fourteen geological horizons with a contour interval of 100 m on the scale of 1:300,000 from Base Zechstein to Base Middle Miocene to Pliocene (Tertiary) are presented. The presentation of the structural situation of the study area is based on this data (Baldschuhn et al. 2001).

A map of the Base Tertiary based on 3D Seismic Data was available for a part of the study area (BEB 2002). A graphical presentation of the map is not possible. Consequently, only derived data were shown (profiles, statistical analyses). The depth information from this high resolutioned map (contour interval of 25 m) was combined with the data from the Base Tertiary of the Geotectonic Atlas of NW-Germany. The geographical position of the map is shown in Fig. 5.

Data collection and spatial analyses

Morphological elements of the modern landscape (fluvial system, holocene alluvial plain, lower weichselian terrace, catchment basin, topography) were vectorised from the historical and modern topographical maps (LGN 1898, 1994), (Fig. 8, step C1). The ground level elevation was mainly vectorised from the modern topographical maps. The historical maps were used only for the reconstruction of artificial modified landscapes during the twentieth century (e.g. high density areas). The ground-level elevation of the investigated part of the River Hunte catchment basin (Fig. 6) was mapped with a contour interval of 1.25 m. Bench marks were vectorisied from the topographical maps and integrated into the process of Digital Elevation Model generation. The structural informations (depth informations of the geological strata, faults, salt structures, outcrops) were vectorised from the Geotectonic Atlas of NW-Germany (Baldschuhn et al. 1996) and the depth of the Base Quaternary from the Geological Map (NLfB 1993)

which shows the depth of the Base Quaternary with a contour interval of 25 m (Fig. 8, step C2).

The vectorised contour lines from the structural/geological and topographical maps form the basis for Digital Spatial Models (DSM) and the Digital Elevation Models (DEM), (Fig. 8, step D2 and D3). All DEMs and DSMs were calculated with the program Arc View 3.2 (Module Spatial Analyst 2.0) with a grid-cell size of 30 m. These Digital Models form the basis for later spatial data requests (depth/height requests [Fig. 8, step E] and calculation of linear correlation coefficients [Fig. 8, step F2]).

Depth/height requests for single segments (Fig. 8, step E) were carried out by calculating the arithmetic mean of grid heights which can be found within the area of single segments. Mean heights of segments of the Lower Weichselian Terrace, the catchment basin and the mean depth of the geological subground were calculated by this method. Mean heights of Holocene Alluvial Plain segments were determined by using height information of contour lines crossing a segment or benchmarks positioned within a segment. The height of Holocene Alluvial Plain segments with no height information from contour lines or benchmarks were determined by linear interpolation between segments with height data. The heights of Holocene Alluvial Plain segments were not calculated directly from the DEM because the density of height information is insufficient within most of the Holocene Alluvial Plain segments. Height requests by GIS would therefore lead to erroneous results for most of the Holocene Alluvial Plain segments.

Results

Correlations between the depth of the geological subsurface and the height of the Holocene Alluvial Plain/Lower Weichselian Terrace

Linear correlation coefficients between the depth of the geological underground and the height of the Holocene Alluvial Plain/Lower Weichselian Terrace for the Hunte catchment basin have been calculated (Fig. 7, Fig. 8, step F2). This was done to investigate the depth/height relationship between the geological subground and the modern river. The Holocene Alluvial Plain of the River Hunte was cut into 177 segments of nearly equal length ~500 m (Fig. 8, step D1) to obtain enough data points for the construction of the longitudinal profiles (Fig. 8, step F1) and geostatistical analyses (Fig. 8, step F2). The mean depth of the geological subsurface was calculated for each of the 177 segments by the GIS from the Spatial Geological Models constructed from the Geotectonic Atlas of NW-Germany (Baldschuhn et al. 1996). The data were used for the construction of a longitudinal profile by plotting the depth of the geological strata against the segment numbers (Fig. 8, step F1). The resulting longitudinal profile is shown in Fig. 9c. Linear correlation coefficients were calculated between the different depth data and are summarized in Table 1.

Linear correlation coefficients were calculated for different segment lengths between the depth of the Base of Tertiary and the height of the Holocene Alluvial Plain. Segment lengths of 250–5,000 m result in a linear correlation coefficient of r^2 between 0.95 and 0.97. Consequently, there is only a minor influx of changing segment lengths on resulting linear correlation coefficients.

Not all of the fourteen geological layers available from the Geotectonic Atlas of NW-Germany (Baldschuhn et al. 1996) were used for the calculation of the linear correlation coefficients, because outcrops cover wide areas of the Base Middle Jurassic, Base Upper Jurassic and the Base Lower Miocene to Pliocene (maps not shown). Thus, no depth information is available from those outcrop parts. Consequently, those three layers were not taken into account for this study. Linear correlation coefficients between the remaining eleven layers of the geological subsurface are shown in the blue coloured cells "A-N" (Table 1). Linear correlation coefficients calculated between the depth at the Base of Quaternary and the depth of the geological subsurface are shown in the green cells "O" (Table 1). Linear correlation coefficients calculated between the height of the Holocene Alluvial Plain and the depth of the geological subsurface are shown in the yellow cells "P" (Table 1). Correlation coefficients of ≥ 0.60 are given in red. The value of ≥ 0.60 serves as an arbitrary threshold to distinguish lower from higher linear correlation coefficients. The mean linear correlation coefficient for the whole blue field (cells A–N) is 0.74 (Table 1). Adjacent geological units are connected by a dashed line. The mean linear correlation coefficient for the adjacent geological units is 0.92, showing that the situation from the deeper geological basement up to the shallower strata is similar. A linear correlation coefficient of 0.95 is visible between the height of the Holocene Alluvial Plain and the depth at the Base of Tertiary (Table 1, cell JP, black arrow). Fig. 10c shows the corresponding XY-plot.

The green column "O" (Table 1) shows the linear correlation coefficients between the Base of Quaternary and the depth of the geological subsurface. All linear correlation coefficients are below 0.39. Consequently, there is no significant correlation between the depth of the Base Quaternary and the geological subsurface. The reason for these low correlation coefficients is the post-depositional erosion of the Elsterian glacial channels into the top of Tertiary (Fig. 9b, black arrows). These glacial channels have cut up to a depth of −200 m a.s.l. into the subground. Thus, the top of the Tertiary sediments is controlled by the incision of the Elsterian glacial channels. Sediments of deeper than −200 m a.s.l. are unaffected by this glacial erosion because these are the deepest detectable Elsterian subglacial channels in the study area (NLfB 1993). This fact applies only to this particular research area. Glacial channels more than 400 m in depth have been described (Kuster and Meyer

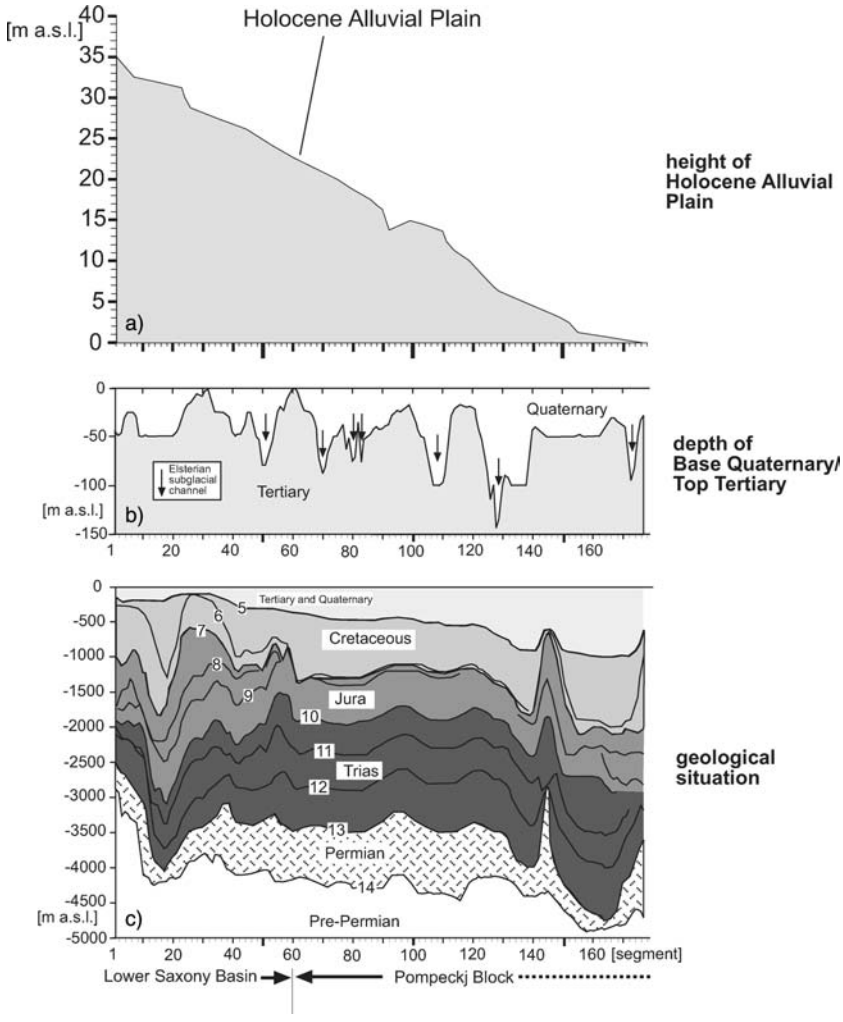

Fig. 9 Longitudinal profile for a part of the River Hunte from south to north with **a** height position of the Lower Weichselian Terrace above the Holocene Alluvial Plain in metre, after historical and modern topographical maps (LGN 1898; LGN 1994), **b** depth at the Base of Quaternary in (m a.s.l.), the *black arrows* show the position of Elsterian tunnel valleys, after Quaternary Geological Map (NLfB 1993), **c** geological situation, depth at the Base of Zechstein (*number 14*) to the Base of Tertiary (*number 5*), after Geotectonic Atlas of NW-Germany (Baldschuhn et al. 1996). The depth at the Base of Tertiary is based on a 3D-seismic data contour map between segment 58–129 and 158–177 (BEB 2002)

1979; Ortlam and Vierhuff 1978). A glacial erosion influence for the Base of Tertiary could therefore be excluded for the study area. The linear correlation coefficients are clearly below 0.6 between the height of the Holocene Alluvial Plain and the depth at the Base Upper Buntsandstein (Table 1, cell "CP", $r^2 = 0.48$), the Base Keuper (Table 1, cell "DP", $r^2 = 0.41$) and the Base Lower Jurassic (Table 1, cell "EP", $r^2 = 0.15$). However, there is a higher linear correlation coefficient of 0.78 between the depth at the Base Zechstein and the height of the Holocene Alluvial Plain (Table 1, cell "AP") and a linear correlation coefficient of 0.66 between the depth at the Base of Lower and Middle Buntsandstein (Table 1, cell "BP"). Consequently, there is a high correlation between the deepest geological basement (Base Zechstein and Base Lower and Middle Buntsandstein), the uppermost geological strata (the depth of the entire Tertiary) and the modern landscape (height of the Holocene Alluvial Plain). It is evident by Fig. 10b that the linear correlation between the height of the Lower Weichselian Terrace and the depth at the Base of Tertiary is 0.95. An explanation for these correlations will be given in discussion.

Correlations between the depth of the geological subsurface and the height of the catchment basin topography

The Hunte catchment basin was divided into 35 segments. A segmentation of the Hunte catchment basin into 177 segments as praticed for the Holocene Alluvial Plain (see Chapter "Correlations between the depth of the geological subsurface and the height of the Holocene Alluvial Plain/Lower Weichselian Terrace") would lead to (1) adaptive difficulties in the curved parts of the River Hunte catchment basin and (2) would result in segment areas too small for reliable geostatistical analysis. The position of the segments is shown in Fig. 7 (segment number 1 is given by the area between segment line1–5, number 2 by the area between segment line 5–10,..., segment number 35 by the area between segment line 170–175). The mean depth of the geological subsurface and the mean topographical height were calculated for each of the 35 segments by the method already described in Chapter "Correlations between the depth of the geological subsurface and the height of the Holocene Alluvial Plain/Lower Weichselian Terrace". Linear

Table 1 Linear correlation coefficients calculated between the height of the Holocene Alluvial Plain and the geological subsurface. The geographical position of the investigated area is shown in Fig. 7. The blue field (cells *A*–*N*) after Geotectonic Atlas of NW-Germany (Baldschuhn et al. 1996) and 3D Seismic contour map of the Base Tertiary (BEB 2002). The green field Base of Quaternary (cell *O*) after the Map of Base Quaternary for Lower Saxony (NLfB 1993). The yellow field Holocene Alluvial Plain (cell *P*) after modern and historical topographical maps (LGN 1898; LGN 1994). For detailed explanation see Chapter "Correlations between the depth of the geological subsurface and the height of the Holocene Alluvial Plain/Lower Weichselian Terrace"

		A	B	C	D	E	F*	G*	H	I	J	K	L	M*	N	O	P
		Base Zechstein	B. L. + Middle Buntsandstein	B. U. Buntsandstein+Muschelk.	Base Keuper	B. L. Jurassic	Base Middle Jurassic*	Base Upper Jurassic*	Base marine Lower Cretaceous	Base Upper Cretaceous	Base Tertiary	B. M. Eocene to Lower Oligocene	B. M. Oligocene to Upper Oligo.	B. Lower Miocene to Pliocene*	B. Middle Miocene to Pliocene	Base of Quaternary	Holocene Alluvial Plain
A	Base Zechstein		0.85	0.75	0.65	0.43			0.69	0.79	0.78	0.77	0.69		0.61	0.19	0.78
B	B. L. + Middle Buntsandstein			0.96	0.90	0.78			0.76	0.70	0.75	0.85	0.79		0.74	0.16	0.66
C	B. U. Buntsandstein+Muschelkalk				0.94	0.88			0.70	0.57	0.58	0.78	0.72		0.68	0.09	0.48
D	Base Keuper					0.93			0.72	0.52	0.53	0.74	0.72		0.71	0.05	0.41
E	Base Lower Jurassic								0.64	0.36	0.30	0.63	0.68		0.69	0.06	0.15
F*	Base Middle Jurassic*																
G*	Base Upper Jurassic*																
H	Base marine Lower Cretaceous									0.86	0.76	0.69	0.68		0.68	0.34	0.61
I	Base Upper Cretaceous										0.85	0.76	0.67		0.64	0.33	0.73
J	Base Tertiary											0.97	0.93		0.90	0.38	0.95
K	B. M. Eocene to Lower Oligocene												0.96		0.94	0.23	0.92
L	B. M. Oligocene to Upper Oligocene														0.97	0.33	0.92
M*	Base Lower Miocene to Pliocene*																
N	Base Middle Miocene to Pliocene															0.34	0.91
O	Base of Quaternary																0.33
P	Holocene Alluvial Plain																

mean of blue field (A-N) = 0.74
mean of adjacent geological units (dashed line) = 0.92
red numbers = linear correlation coefficient >= 0.60

blue field, cells "A-N" after Baldschuhn et al. (1996) and BEB (2002)
green field, cell "O" (Base of Quaternary) after NLfB (1993)
yellow field, cell "P" (Holocene Alluvial P.) after LGN (1898 and 1994)

*linear correlation coefficients for layer F, G, M not shown, for explanation see Chapter "Correlations between the depth of the geological subsurface and the height of the Holocene Alluvial Plain/Lower Weichselian Terrace"

correlation coefficients have been calculated based on the depth/height data (Table 2). Similarities and differences between Table 1 and 2 will be dealt with. There is the same high mean linear correlation coefficient ($r^2 = 0.93$) between adjacent geological units as shown for the segments of the Holocene Alluvial Plain (Table 1, $r^2 = 0.92$), indicating that the structural situation from the deeper geological basement up to the shallower strata is very similar. There are high linear correlation coefficients between the depth at the Base of Quaternary and the depth of Tertiary (Table 2, cell "JO", $r^2 = 0.63$; cell "KO", $r^2 = 0.86$; cell "LO", $r^2 = 0.92$; cell "NO", $r^2 = 0.92$) and the height of the modern catchment basin topography (Table 2, cell "OP", $r^2 = 0.84$, black arrow). There are high linear correlation coefficients between the height of the catchment basin topography, the depth at the Base Zechstein (Table 2, cell "AP", $r^2 = 0.67$) and the depth at the Base Lower and Middle Buntsandstein (Table 2, cell "BP", $r^2 = 0.69$) and the depth of the Tertiary (Table 2, cell "JP" $r^2 = 0.87$, cell "KP" $r^2 = 0.95$, cell "LP" $r^2 = 0.97$, cell "NP" $r^2 = 0.95$). The XY-plot of Fig. 10 a shows that the correlation between the depth at the Base of Tertiary and the height of the catchment basin topography is $r^2 = 0.87$. Thus, the modern topography is clearly correlated with the morphology of the deep geological structures.

Correlations between the depth of basement blocks and the height of topography

Figure 11 shows the pattern of basement blocks for a part of the river Hunte catchment basin. Eight basement blocks are signed with the letters B, C, D, E, F, G, H and I, shown also in Fig. 3. Basement blocks C and D were combined to a single block. The mean topographical height of these seven blocks was determined with the GIS. The resulting mean heights are given in m a.s.l.. The gray tones of the individual blocks correspond to the mean topographic from white (E) = 43.4 m to black (B) = 8.2 m (Fig. 11). The basement block E (Bockstedt Graben Lessen-Staffhorst-Block) shows the highest average topographical height of 43.4 m. This block is 5.4 m higher than the southerly positioned Oythe-Düste-Wehrbleck-Block (F) and 14.5 m higher than the northerly adjacent Südoldenburg Block (C, D). Base-

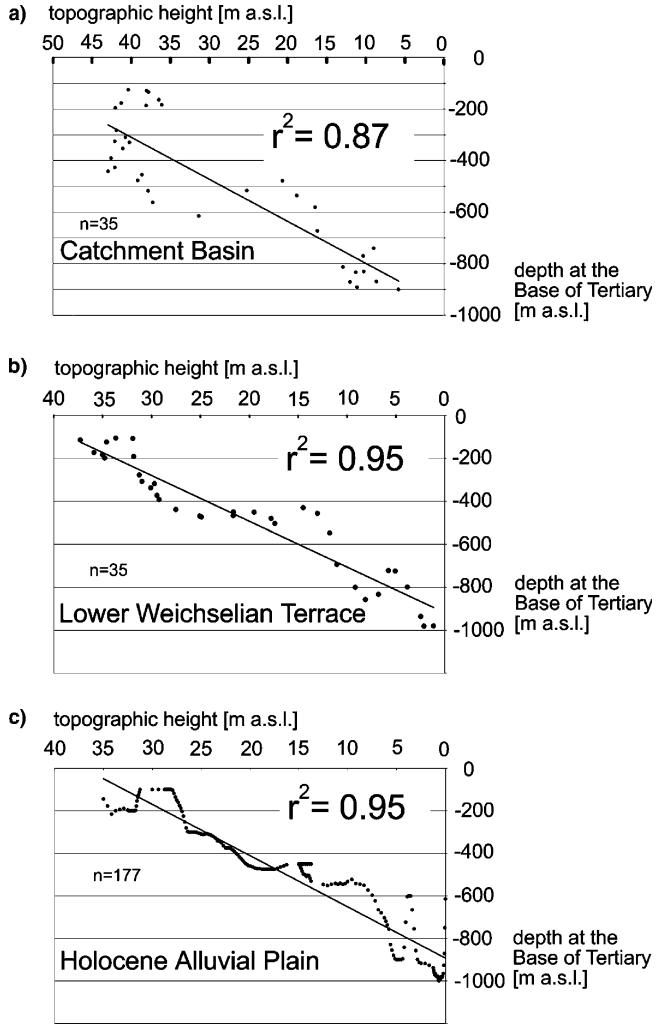

Fig. 10 XY-plots for a part of the River Hunte catchment basin. Depth at the Base of Tertiary against the topographic height of **a** the catchment basin, **b** the Lower Weichselian Terrace and **c** the Holocene Alluvial Plain. Regression line and linear correlation coefficient are presented for all diagrams. The geographical position of the investigated catchment basin is shown in Fig. 7. For more explanation see Chapter "Correlations between the depth of the geological subsurface and the height of the Holocene Alluvial Plain/Lower Weichselian Terrace" and "Correlations between the depth of the geological subsurface and the height of the catchment basin topography". After historical and modern topographical maps (LGN 1898; LGN 1994), Tectonic Atlas of NW-Germany (Baldschuhn et al. 1996) and 3D Seismic contour map of Base Tertiary (BEB 2002)

ment block E separates the Lower Saxony Basin in the south from the northerly adjacent Pompeckj Block. Fig. 12a–h shows XY-plots between the average topographical height of the basement blocks and the average depth of the geological basement. The highest correlation of $r^2 = 0.92$ is visible between the topography and the depth at the Base of Tertiary (Fig. 12a). The lowest correlation of $r^2 = 0.55$ is presented by the Base of Lower Jurassic (Fig. 12d). All linear correlation coefficients for the deepest parts of the Basin are higher than $r^2 = 0.71$ (between the Base of Keuper [Fig. 12e] and the Base of Zechstein [Fig. 12h]). The Base of Lower and Middle Buntsandstein (Fig. 12g) shows correlation of $r^2 = 0.81$ – the highest linear correlation coefficient.

Correlations between the depth of the geological subsurface and the watershed topography

Topographical- and geological profiles have been constructed for the west and eastside of the watershed (Fig. 13, left and right). The geographical position of the watershed profiles is shown in Fig. 4 (profile AB, Fig. 13, left, and profile CD, Fig. 13, right).

Linear correlation coefficients have been calculated between the westside watershed topography and the depth of the geological subground (Base Tertiary and the Base of Upper Cretaceous). The profile for the westward watershed is shown in Fig. 13, left. The calculated linear correlation coefficients are summarized in Table 3. The linear correlation coefficient between the topography and the depth at the Base Tertiary is 0.71 (Table 3, cell "AB"); between the depth at the Base Tertiary and the depth at the Base of Upper Cretaceous 0.91 (Table 3 cell "BC"); and between the depth at the Base of Upper Cretaceous and the topography 0.63 (Table 3 cell "AC"). Consequently, there is a positive correlation for the westside watershed between the depth of the geological subsurface and the topography.

The linear correlation coefficients for the eastside watershed are shown in Table 4. The profile is shown in Fig. 13, right. The linear correlation coefficient between the topography and the depth at the Base Tertiary is 0.74 (Table 4, cell "AB"); between the depth at the Base Tertiary and the depth at the Base of Upper Cretaceous 0.57 (Table 4, cell "BC"); and between the depth at the Base of Upper Cretaceous and the topography −0.03 (Table 4, cell "AC"). Thus, there is no significant correlation between the topography and the depth at the Base of Upper Cretaceous, but between the depth at the Base of Tertiary and the depth at the Base of Upper Cretaceous.

The mean topographic height of the westside watershed is 29.90 m, and 42.80 m for the eastside (Fig. 13a, left and right, bold dashed line). Thus, the mean eastside topography is ∽13.00 m higher than the westside (Fig. 13b left and right, bold dashed line). The westside shows a mean depth at the Base of Tertiary of −640 m, and the eastside of −410 m. Thus, the eastside Base of Tertiary is 230 m more elevated than the westside (Fig. 13b left and right, bold dashed line). A similar picture is visible at the Base of Upper Cretaceous. Here, the westside shows a mean depth of −1,350 m, the eastside of −1,020 m (Fig. 13b left and right, bold dashed line). Consequently, the eastside watershed topography and geological subsurface is higher than that of the westside.

Discussion

The study area is covered by Quaternary sediments. Sediments have the potential to record the youngest

Table 2 Linear correlation coefficients calculated between the modern topography and the geological subsurface for segments of the Hunte catchment basin. The geographical position of the investigated area is shown in Fig. 7. The blue field (cells *A–N*) after Geotectonic Atlas of NW-Germany (Baldschuhn et al. 1996) and 3D Seismic contour map of the Base Tertiary (BEB 2002). The green field Base of Quaternary (cell *O*) after the Map of Base Quaternary for Lower Saxony (NLfB 1993). The yellow field Holocene Alluvial Plain (cell *P*) after modern and historical topographical maps (LGN 1898; LGN 1994). For detailed explanation see Chapter "Correlations between the depth of the geological subsurface and the height of the catchment basin topography"

		A	B	C	D	E	F*	G*	H	I	J	K	L	M*	N	O	P
		Base Zechstein	B. L. + Middle Buntsandstein	B. U. Buntsandstein+Muschelk.	Base Keuper	B. L. Jurassic	Base Middle Jurassic*	Base Upper Jurassic*	Base marine Lower Cretaceous	Base Upper Cretaceous	Base Tertiary	B. M. Eocene to Lower Oligocene	B. M. Oligocene to Upper Oligo.	B. Lower Miocene to Pliocene*	B. Middle Miocene to Pliocene	Base of Quaternary	Modern Topography
A	Base Zechstein		0.94	0.87	0.76	0.56			0.79	0.66	0.75	0.73	0.63		0.62	0.34	0.67
B	B. L. + Middle Buntsandstein			0.97	0.92	0.77			0.79	0.51	0.71	0.76	0.63		0.60	0.39	0.69
C	B. U. Buntsandstein+Muschelkalk				0.96	0.87			0.72	0.34	0.55	0.68	0.54		0.51	0.30	0.58
D	Base Keuper					0.93			0.63	0.25	0.49	0.71	0.56		0.53	0.35	0.57
E	Base Lower Jurassic								0.51	0.08	0.25	0.66	0.51		0.48	0.26	0.39
F*	Base Middle Jurassic*																
G*	Base Upper Jurassic*																
H	Base marine Lower Cretaceous									0.84	0.76	0.59	0.46		0.47	0.33	0.58
I	Base Upper Cretaceous										0.85	0.63	0.53		0.55	0.34	0.56
J	Base Tertiary											0.97	0.91		0.91	0.63	0.87
K	B. M. Eocene to Lower Oligocene												0.96		0.95	0.86	0.95
L	B. M. Oligocene to Upper Oligocene														0.99	0.92	0.97
M*	Base Lower Miocene to Pliocene*																
N	Base Middle Miocene to Pliocene															0.92	0.95
O	Base of Quaternary																0.84
P	Modern Topography																

mean of blue field (A-N) = 0.67
mean of adjacent geological units (dashed line) = 0.93
red numbers = linear correlation coefficient >= 0.60

blue field, cells "A-N" after Baldschuhn et al. (1996) and BEB (2002)
green field, cell "O" (Base of Quaternary) after NLfB (1993)
yellow field, cell "P" (Modern Topography) after LGN (1898 and 1994)

*linear correlation coefficients for layer F, G, M not shown, for explanation see Chapter "Correlations between the depth of the geological subsurface and the height of the Holocene Alluvial Plain/Lower Weichselian Terrace"

tectonic movements (Sirocko et al. 2002; Vanneste et al. 1999), but are on the other hand easily erodable, which could lead to the destruction of "neotectonic/active tectonic fingerprints" during times of lower tectonic activity or even quiescence. However, there is no indication of tectonic quiescence in northern Europe during the Quaternary as suggested by studies dealing with fluvial terrace warping (e.g. Houtgast et al. 2002; Maddy et al. 2000), subsidence analyses (e.g. Geluk et al. 1994; Houtgast and van Balen 2000), recent seismicity (e.g. Camelbeeck and Meghraoui 1996; Grünthal and Stromeyer 2001; Leydecker and Kopera 1999; Leydecker et al. 1980), lineament analyses (e.g. Dulce and Gronemeier 1982; Kronberg 1991; Krull et al. 1985; Krull and Wegner 1988; Sesören 1976) and geodetic relevelling data (e.g. Bankwitz 1976; DGK-Arbeitskreis 1979; Frischbutter 2001; Ihde et al. 1987; Kooi et al. 1998; Leonhard 1988; Schwab 1981; Schwab et al. 1973; Wübbelmann 1993). In contrast, the long term trend of neotectonic movements, which is evident for middle and northern Europe beginning in the early Oligocene (Rupelian stage, ~37 Ma), (Ludwig 2001a), seems to intensify during Pliocene/Pleistocene times. This is evident by an increase in subsidence (Geluk et al. 1994; Houtgast and van Balen 2000; Kooi et al. 1989, 1991; Thorne and Watts 1989; Zagwijn 1989) which is thought to be caused by a process of plate reorganization (Cloetingh et al. 1990). An abruptly accelerated uplift of the Rhenish Massif is evident since about 800,000 years ago (Meyer and Stets 1998), whereas the North Sea basin strongly subsided during the Quaternary as evident by local sediment thicknesses of up to 1,000 m in the area of the southern Central Graben (Caston 1977). Displacements of marine and lacustrine Holsteinian interglacial sediments in the coastal zone of the North Sea/Baltic Sea and the highland regions in the south are in the order of a few decametres, showing that neotectonic movements continued during the post Holsteinian (Ludwig 2001b).

Correlations between the depth of the geological strata and the height of the modern topography

There is evidence of tectonic geomorphology in the NW-German Basin, as shown in this study by correlations

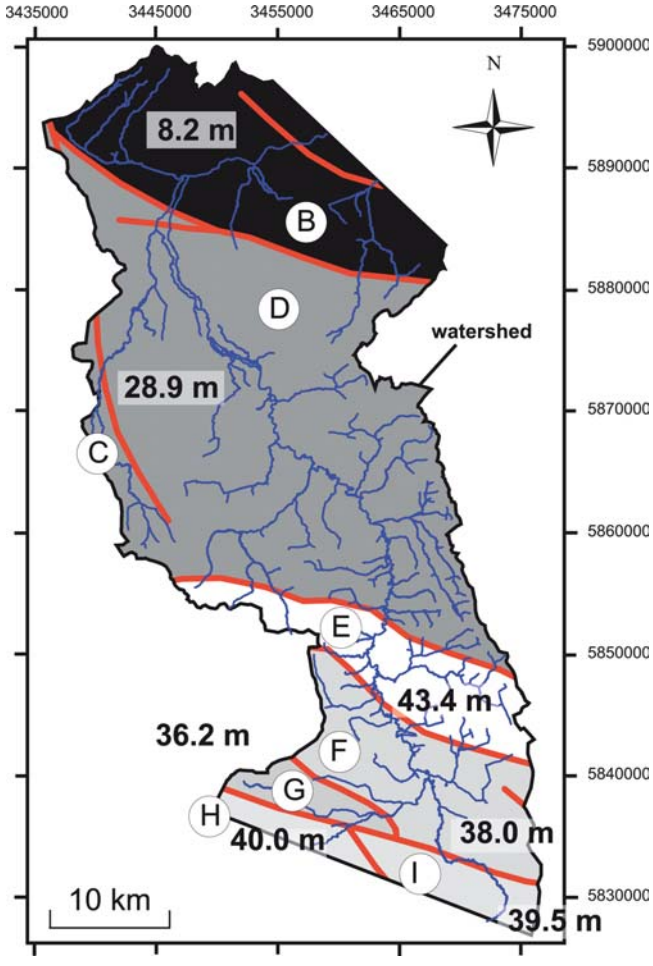

Fig. 11 Pattern of basement blocks for the investigated part of the River Hunte catchment basin, after Tectonic Atlas of NW-Germany (Baldschuhn et al. 2001). The letters *B–I* indicate the names of the basement blocks. The names are given in Fig. 3. The fluvial system is shown in *blue*, after historical topographical map (LGN 1898)

between the height of modern landscape and the depth of the geological subground, which will be discussed in following sections in more detail.

To investigate the depth/height relationship between the geological subground and the modern topography, linear correlation coefficients have been calculated (Table 1, 2, 3, 4; Fig. 10, Fig. 12). A connection between the modern landscape and the geological subground is proven by the high linear correlation coefficients. What causes these high correlations? A non-tectonic and a tectonic mechanism are probable causes. The depth at the Base of Tertiary increases from about −200 in the south to −1,000 m a.s.l in the north. The same northward orientated gradient is shown by the Hunte (Fig. 9a, c). Potentially, the sedimentary fill of the basin's deeper parts in the north is still not finished. Thus, the S–N gradient could be caused by a non-compensated paleorelief which forces the Hunte to flow in a northerly direction. After this non-tectonic model, the correlation between the depth at the Tertiary strata and the height of the Holocene Alluvial Plain is caused by a pure exogenic process of sedimentary fill of the given paleorelief without any tectonic influx on sedimentation.

Unlike the exogenic scenario (see above) one could also interpret that the active tilting of the basin forces the Hunte to flow northward. There is evidence for Cenozoic tectonic subsidence in the North Sea Basin and uplift of the adjacent mainland. Fig. 14 shows that the Central Graben of the North Sea is a depocentre for Cenozoic sediments (Ziegler 1990).

The thickness of all Tertiary sediments increases towards the Central Graben and more than 3,600 m of compacted sediments have been deposited in this axial zone, of which 1,600 m alone have been deposited during the time span of Middle Miocene to Quaternary (Kockel 1988), (Fig. 15).

Up to 1,000 m of Quaternary sediments have been deposited at the southern tongue of the Central Graben with a mean subsidence rate of about 0.5 mm/a (deposition of about 1,000 m of Quaternary sediments over a time span of 1.8 Ma), (Caston 1977), (Fig. 16).

The subsidence rate in the southern part of the North Sea area accelerates during the Late Pliocene and Quaternary (Kooi et al. 1989, 1991; Thorne and Watts 1989; Zagwijn 1989). This acceleration of subsidence in the North Sea Central Graben occurred well before the onset of the Quaternary with a tenfold increase during the Late Pliocene relative to previous Tertiary rates (Kooi et al. 1991). The large Pliocene-Quaternary sediment thickness in the southern North Sea Basin is not caused by sediment infill of a Pliocene deep-water basin as suggested by Sclater and Christie (1980), because sediment infill is shallow marin (littoral and epineretic) or of continental facies (Kooi et al. 1991). Subsidence and sedimentation rates were nearly in equilibrium, whereas subsidence never became so rapid to cause water depths of considerably more than 100 m (Zagwijn 1989).

Figure 17 shows the most important European areas of subsidence and uplift (I–VII) since the beginning of Rupelian stage (~37 Ma), (Ludwig 2001a), characterised from the IGCP Project 346 Neogeodynamica Baltica (Stackebrandt et al. 2001). Neogeodynamic activities of the Baltic Sea depression and its southern surrounding were derived from the position of reference horizons (deposits of the Early Oligocene, Base of Quaternary, surface of the Holsteinian interglacial/Saalian glacial river terraces). The study area (grey rectangle) is situated between the zone of Central European uplift (V) in the south and the zone of Central European depression (III, green line) in the north, forming a NW-SE striking trough-like subsidence zone, which extends from the strongly subsiding North Sea to southern Poland. Fig. 18 shows a longitudinal profile from the Osnabrücker Bergland (A) in the south over the North Sea coastal zone in the north (B) to the centre of Cenozoic subsidence at the North Sea Central Graben in the NW (C). The position of the profile which crosses the study area between profile point AB is shown in Fig. 15.

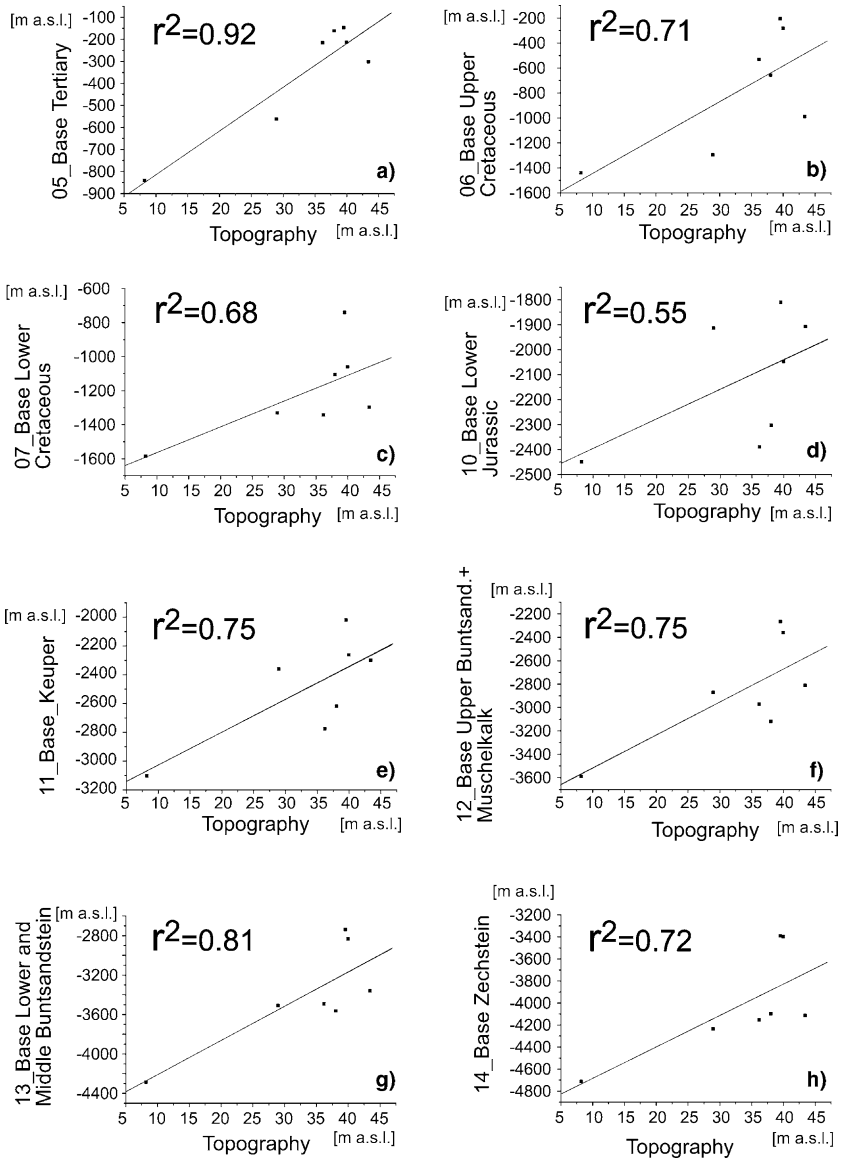

Fig. 12 *XY*-plots. Mean topographical height of basement blocks (Fig. 11) against the **a** Base of Tertiary, **b** Base Upper Cretaceous, **c** Base Lower Cretaceous, **d** Base Lower Jurassic, **e** Base Keuper, **f** Base Upper Bundsandstein + Muschelkalk, **g** Base Lower and Middle Buntsandstein and **h** Base Zechstein (Permian) with regression lines and linear correlation coefficients (r^2)

Relicts of Early to Middle Miocene marine deposits can be found in the area of the Osnabrücker Bergland (Wiehengebirge) at a height of about +100 m a.s.l. (Anderson and Indans 1969; Haack 1932; Hiltermann 1984; Hinsch et al. 1978; Hinze 1979; Thiermann 1970). At the West-Schleswig Jade Trough, the depth of the Base Middle Miocene is about −1,000 m (Fig. 15, red circle 1 and Fig. 18) and at the centre of the North Sea Central Graben about −1,600 m (Fig. 15). The geological profile of Fig. 18 shows that the height difference of the Base Middle Miocene between the Osnabrücker Bergland in the south and the Central Graben in the north is about 1,700 m and between the Osnabrücker Bergland and the West-Schleswig Trough about 1,100 m. This increase of depth in a northerly direction cannot be explained by changes of the paleo-bathymetry alone, because Middle Miocene sediments were deposited under shallower marine conditions (Hinsch and Ortlam 1974). The relicts of Early to Middle Miocene sediments, which can be found in the area of the Osnabrücker Bergland prove that the Middle Miocene sea extended to the area of the Osnabrücker Bergland and probably even connected the North Sea with the Upper Rhine valley (Hinsch et al. 1978). Post-Middle Miocene uplift of the hinterland led to erosion of the formerly deposited marine sediments (Fig. 18, between profile distance 0–80 km), (Hinsch and Ortlam 1974). This uplift continued during the Pliocene which led to sculpturing of the formerly low relief land surfaces (Gramann and Kockel 1988). Whilst the hinterland was uplifted, the West-Schleswig-Jade Trough, which can be found north of the estuary mouth of the Rivers Weser and Elbe (Fig. 15, 16, 18), subsided strongly during the Miocene and continued to subside during the Pliocene (Gramann and Kockel 1988). The West-Schleswig-Jade Trough was strongly affected by halocinetic movements as evident by the formation of deep rim synclines (Baldschuhn et al. 2001). The different rate of subsidence

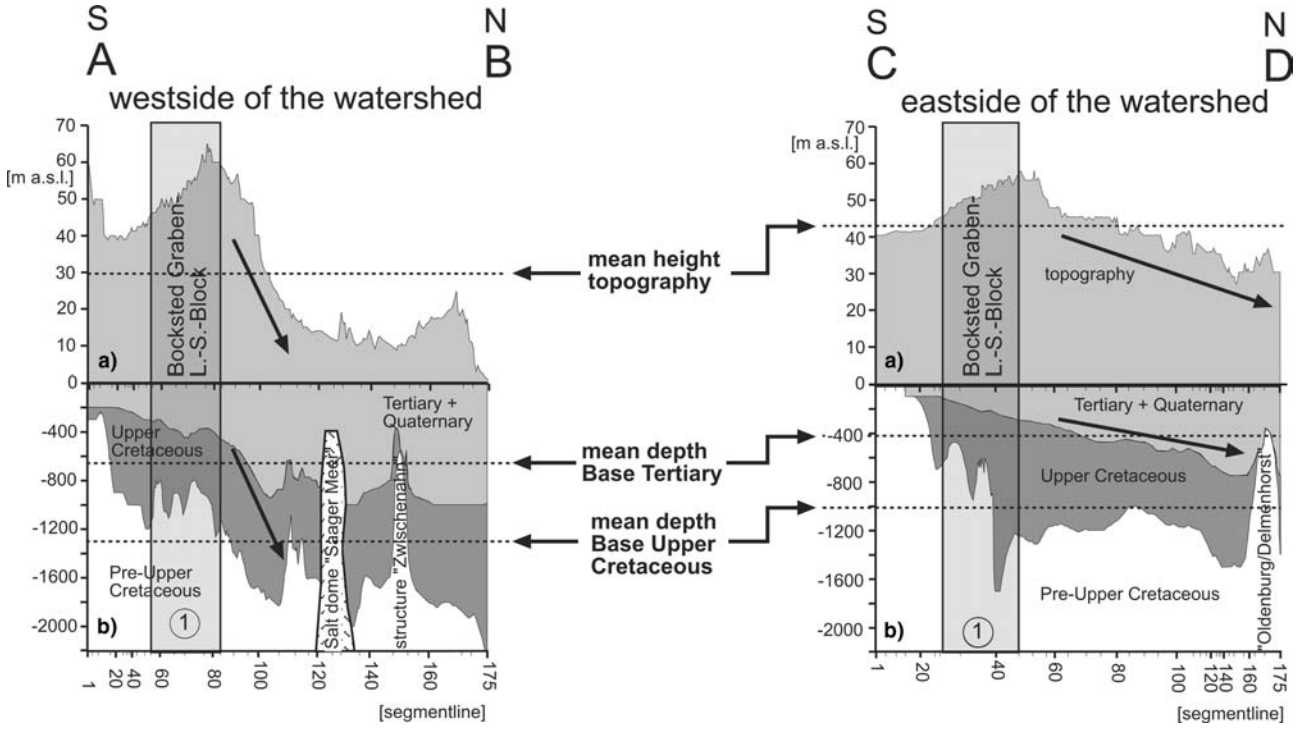

Fig. 13 *Left*: longitudinal profile (AB) for the westside watershed of the River Hunte from south to north with **a** topography, based on historical and topographical maps (LGN 1898; LGN 1994), **b** depth at the Base of Tertiary and the Base Upper Cretaceous after Geotectonic Atlas of NW-Germany (Baldschuhn et al. 1996) and 3D Seismic contour map of the Base Tertiary (BEB 2002). Grey marker 1 shows the position of the Bockstedt Graben Lessen-Staffhorst-Block. The geographical position of this Block is given in Fig. 3, letter *E*. The geographical position of the profile is presented in Fig. 4. *Right*: longitudinal profile (CD) for the eastside watershed of the River Hunte from south to north with **a** topography, based on historical and topographical maps (LGN 1898; LGN 1994), **b** depth at the Base of Tertiary and the Base Upper Cretaceous after Geotectonic Atlas of NW-Germany (Baldschuhn et al. 1996) and 3D Seismic contour map of the Base Tertiary (BEB 2002). Grey marker 1 shows the position of the Bockstedt Graben Lessen-Staffhorst-Block. The geographical position of this Block is given in Fig. 3, letter *E*. The geographical position of the profile is presented in Fig. 4

of blocks in the pre-Permian basement locally shows increases due to salt migration from the rim sinks into the salt structures (Hinsch 1988).

There is evidence for neotectonic movement in the area of the North Sea and the coastal zone of the Baltic sea from height changes of marine Holsteinian and Eemian deposits during the Quaternary. Height differences of the top of marine Holsteinian are about 100 m between the North Sea and the Baltic Sea coast, which result in a mean velocity of about 0.1 mm/a since the End of the Holsteinian Interglacial (Ludwig and Schwab 1995). Post-Eemian crustal movements are proved by dislocations of Eemian marine terraces and deposits in the area of the marginal southern North Sea. A mean deformation rate of about 0.17 mm/a is evident by a maximal height difference of 20.5 m since the end of the Eemian (Streif 1991). This rate is very similar to that of the long-term subsidence rate of The Netherlands which is about 0.14 mm/a since the Eemian (Zagwijn 1983). Streif (1991) suggests that a process of glacial rebound is responsible for the observable post-Eemian crustal movements in the North Sea area. Whilst the southern North Sea area subsided with maximal 0.50 mm/a over the past 1,800 ka (Fig. 16, 19a), the Rhenish Shield was uplifted over the last 800 ka with a mean vertical velocity rate of about 0.25 mm/a as evident by a maximum uplift of about 200 m of the Younger Main Terrace (Meyer and Stets 1998), (Fig. 19g). Fig. 16 shows contour isolines of recent crustal movements (green) which are crossing the study area (red rectangle), (determined from repeated precise levelling data), (after DGK-Arbeitskreis 1979). A northward-oriented gradient of increasing subsidence is visible from about 0 mm/a at the southern border of the study area near the Osnabrücker Bergland to −0.4 mm/a at the northern part near the coastal line of the North Sea. This northward-oriented gradient of modern crustal movements fits well with the long term observed post-Miocene northward tilting (Fig. 18).

The examples given above demonstrate that crustal movement in the North Sea and marginal regions have persisted over the entire Cenozoic period until today. Consequently, there is no evidence for tectonic quiescence during the Tertiary and Quaternary. Thus, it seems unlikely that the high correlations between the depth of the Tertiary strata and the modern topography were caused by a pure exogenic process of sedimentary fill of the given paleorelief without any tectonic influx on sedimentation. More likely, a process of northward tilting caused by uplift of the hinterland (Wiehengebirge [Osnabrücker Bergland]/

Table 3 Linear correlation coefficients calculated between the westside watershed topography (yellow field, cell *A*), the Base of Tertiary (blue field, cell *B*) and the Base of Upper Cretaceous (blue field, cell *C*). After the longitudinal profile (AB) for the westside watershed of the River Hunte (Fig. 13, left). For detailed explanation see Chapter "Correlations between the depth of the geological subsurface and the watershed topography"

		A	B	C
		Topography	Base Tertiary	B. U. Cretaceous
A	Topography		0.71	0.63
B	Base Tertiary			0.91
C	B. U. Cretaceous			

Rhenish Massif) and subsidence of the North-Sea area persists until today and forces the river Hunte to flow in a northerly direction.

Potential driving mechanism for active tectonics in the NW-German Basin

It is evident from the distribution of the global seismicity that the majority of earthquakes is concentrated in the narrow belts of currently active plate boundaries. However, crustal deformation also occurs in the interior of the plates as evident by intraplate seismicity and geodetic measurements of vertical and horizontal crustal movements caused by crustal loading and epeirogeny processes (Brown and Reilinger 1986; Harrison et al. 1999; Nelson et al. 1999; Talwani 1999). Two endogenic forces, (1) crustal rebound (glacial unloading of the Weichselian ice cap) and (2) plate-tectonic processes caused by [a] convergence of Africa–Eurasia, [b] North Atlantic sea-floor spreading (ridge-push), have the most potential to cause active crustal movements inside the NW-German Basin.

Glacial isostatic rebound

It is evident by repeated precise levelling data from Fennoscandia that the region is still subject to vertical uplift, caused by post-glacial rebound of the earth crust (Bakkelid 1986; Sharma 1984), (Fig. 20, yellow isolines). Recent geodetic measurements (Global Positioning system [GPS], Very Long Baseline Interferometry [VLBI]) confirm the results of these earlier works on crustal uplift (James and Lambert 1993; Milne et al. 2001). GPS measurements show a maximum uplift rate of 11.2 ± 0.2 mm/a at the centre of doming at the site Umea (Sweden) and even a tangential (horizontal) divergence away from the centre of uplift in the order of $\sim$1.0 mm/a (Milne et al. 2001). The glacio-isostatic adjustment of Fennoscandia enables modelling of the elastic flexing of the lithosphere, the viscous flow of the mantle and the study of processes associated with this crustal uplift like fracture formation, fault instability, seismicity and changes of the stress field inside and outside the formerly glaciated areas (Grollimund and Zoback 2000; Gudmundsson 1999; Johnston et al. 1998; Klemann and Wolf 1998;

Table 4 Linear correlation coefficients calculated between the eastside watershed topography (yellow field, cell *A*), the Base of Tertiary (blue field, cell *B*) and the Base of Upper Cretaceous (blue field, cell *C*). After the longitudinal profile (CD) for the westside watershed of the River Hunte (Fig. 13, right). For detailed explanation see Chapter "Correlations between the depth of the geological subsurface and the watershed topography"

		A	B	C
		Topography	Base Tertiary	B. U. Cretaceous
A	Topography		0.74	-0.03
B	Base Tertiary			0.57
C	B. U. Cretaceous			

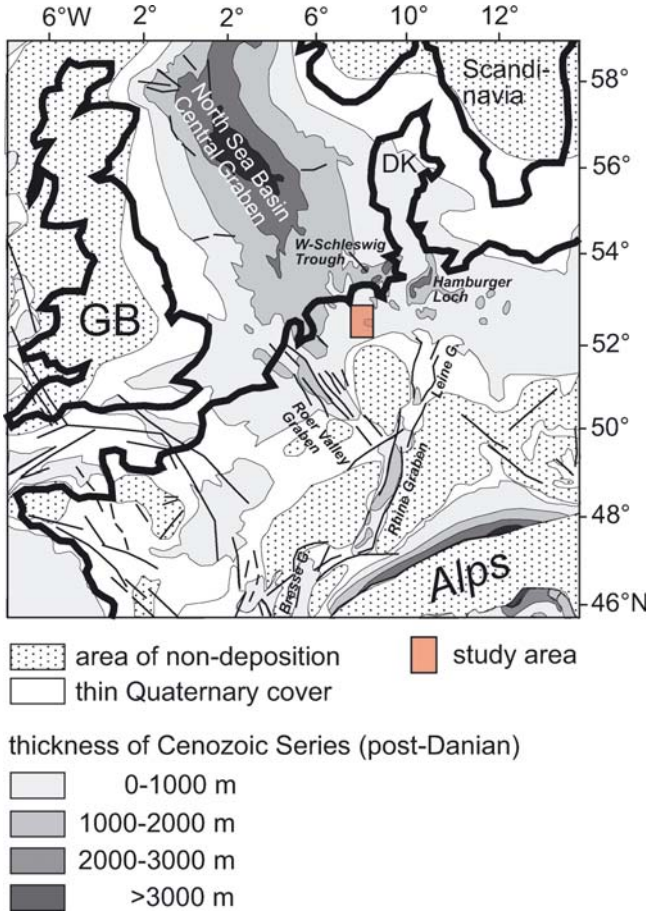

Fig. 14 Thickness of Cenozoic sediments (post Danian) from 0 to >3000 m, after Geological Atlas of Western and Central Europe, (Ziegler 1990). The position of the study area is given by the *red rectangle*

Lagerbäck 1990; Steward et al. 2000; Wahlström 1993; Wolf 1986, 1987, 1993, 1996; Wu et al. 1999; Zoback and Grollimund 2001). The recent generation of rebound models show that horizontal stresses can be transmitted over several hundred kilometres outside the formerly glaciated regions (i.e. well into northern Germany) and that these stresses are able to cause crustal deformation, fault instability and seismicity (James and Lambert 1993; Johnston et al. 1998; Klemann and Wolf 1998; Mitrovica et al. 1994; Wu et al. 1999). Figure 20 shows that the study area (red rectangle) is ~150 km away from the maximum extent of the Weichselian ice sheet during the last glacial maximum (LGM) about 20 ka BP. Consequently, the study area could be influenced by processes of glacio-isostasy during both the glaciated Weichselian and the deglaciated Holocene time. During glacial times, upper-crustal flexural upwarping occurs in the area of the ice-free foreland within the surrounding forebulge rim due to in-migration of sub-crustal material exuded from below the ice sheet (Steward et al. 2000). During deglaciation, the formerly glaciated area shows crustal uplift caused by the removal of the ice load which leads to elastic rebound, faulting and seismicity (Steward et al. 2000). Ductile flow of mantle material inside the formerly glaciated region must lead to a mass deficit in the area outside and possibly to a downwarping of the crust. It is evident by geodetic measurements (Fig. 20) that the process of crustal uplift of Fennoscandia is still going on and that NW-Germany is subsiding probably caused by migration of mantel material into the area of recent Fennoscandian uplift.

Plate tectonic processes, plate velocities and stresses in the lithosphere

Africa and Eurasia are still subject to convergence as evident from plate velocities which were derived from magnetic seafloor-spreading anomalies over a time span of the last 3 Ma and earthquake slip vectors (DeMets et al. 1990, 1994; Minister 1978). The counter clockwise rotation of Africa, which results in a north to north-westward-directed push against Eurasia, is caused by the higher spreading rate of the South Atlantic (~40 mm/a) compared with the lower one of the North Atlantic (~20 mm/a), which leads to a recent lithospheric shortening of about 5–6 mm/a in the area of the Mediterranean (Fig. 20, big red arrow). Based on the evidence from the seafloor-spreading rates, present day seismicity of the Mediterranean region clearly outlines the collision zone between Africa and Eurasia (USGS 2002). Current geodetic measurements of horizontal crustal movements based on space techniques ([VLBI], [GPS], Satellite Laser Ranging Measurements [SLR]) are in a good agreement with the present understanding of the geodynamic situation of the Mediterranean and central Europe (Anzidei et al. 2001; Bastos et al. 1998; Devoti et al. 2002; Kahle et al. 1998; Reilinger et al. 1997). VLBI data shows that southern Italy moves at maximal ~3 mm/a northward (Fig. 20, small red arrows) which results in a northward-orientated compressional strain between the VLBI-station Medicina (Italy) and Wetzell (Germany), (Campell and Nothnagel 2000; Haas et al. 2000). This general compressive stress field postulated by the VLBI-data is consistent with local GPS-measurements from the region of the southern and western Alps, which indicate a north–south shortening at rates of about 1–2 mm/a (Ferhat et al. 1998; Sue et al. 2000).

The World Stress Map Project has shown that these compressive lithospheric stresses can be transmitted from the plate boundaries over great distances into the continental and oceanic domains (Zoback 1992; Zoback et al. 1989). The observed European broad-scale stress field could be simulated by modelling the North Atlantic seafloor-spreading in combination with the northward-directed motion of the African Plate (Gölke and Coblentz 1996; Grünthal and Stromeyer 1992) and Richardson (1992) has shown for North America, western Europe and South

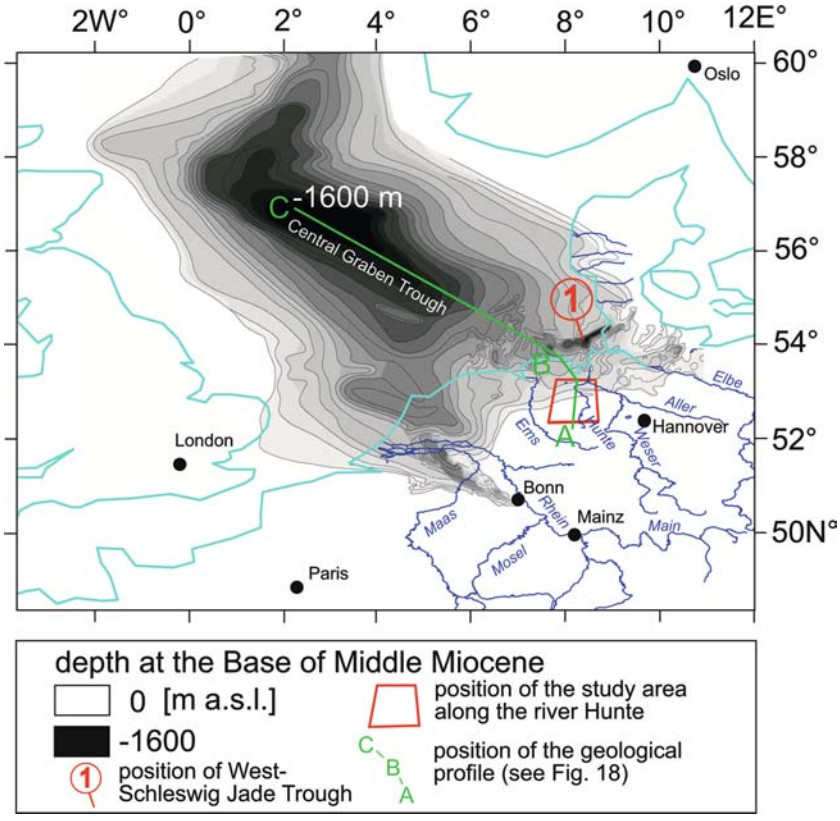

Fig. 15 Depth of the Base Middle Miocene from 0 (*white*) to −1600 m a.s.l. (*black*) after Kockel (1988). The position of the study area is given by the *red rectangle* and the position of the profile ABC by the *green line* (see Fig. 18)

America that the ridge torque correlates strongly with the absolute velocity of the plates and the intraplate stresses. Consequently, there is great accordance between the direction of recent horizontal crustal movements (based on geodetic observations [VLBI, GPS]), the estimates of current plate motions (based on global plate motion models [NUVEL 1A]) and the orientation of the modern stress field (World Stress Map Project). Nevertheless, there is still a debate as to which way the compressional stress field influences sedimentary basins (Cloetingh et al. 1995; Cloetingh et al. 1996, 1994, 1997, 1993; Kooi and Cloetingh 1989; Marshak et al. 1999; Ziegler et al. 1995; Zoback et al. 1993). One scenario which is still under discussion is lithospheric folding which causes broad-scale negative and positive deflections of the lithosphere and leads to upwarping of broad arches and basin subsidence (Bird and Gratz 1990; Burov et al. 1993; Cloetingh and Kooi 1992; Kooi et al. 1989; Kooi et al. 1991; Nikishin et al. 1993; van Wees and Cloetingh 1996). The modern stress field of NW-Europe which

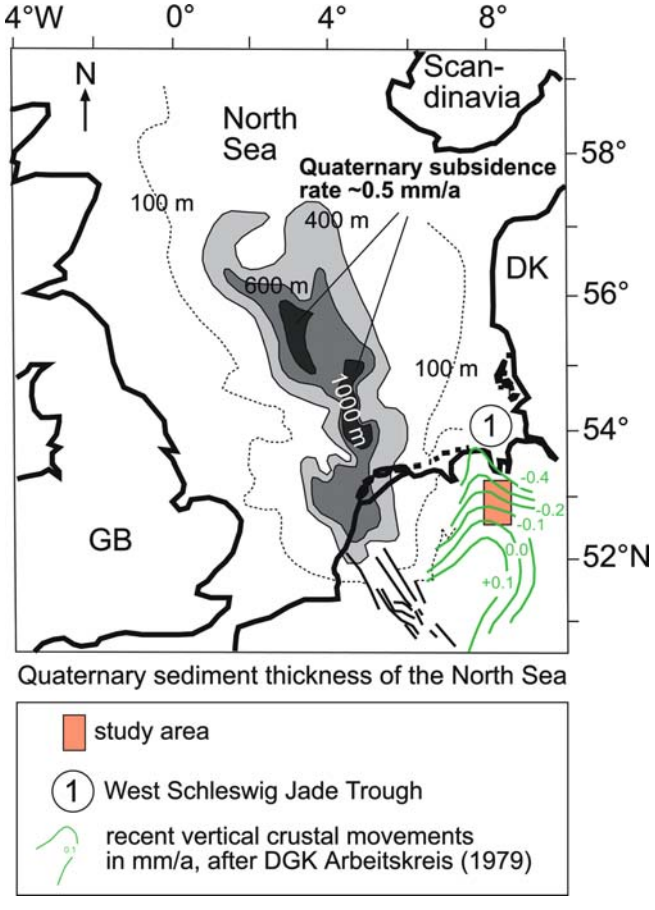

Fig. 16 Thickness of Quaternary sediments of the Southern North Sea from 100 m (*dashed line*) to 1000 m (*black*), (after Caston 1977); the *circled number 1* gives the position of the West-Schleswig-Jade Trough, position of the study area is given by the *red rectangle*, the *green isolines* show the rate of recent vertical movements from +0.1 to −0.4 mm/a (after DGK-Arbeitskreis 1979)

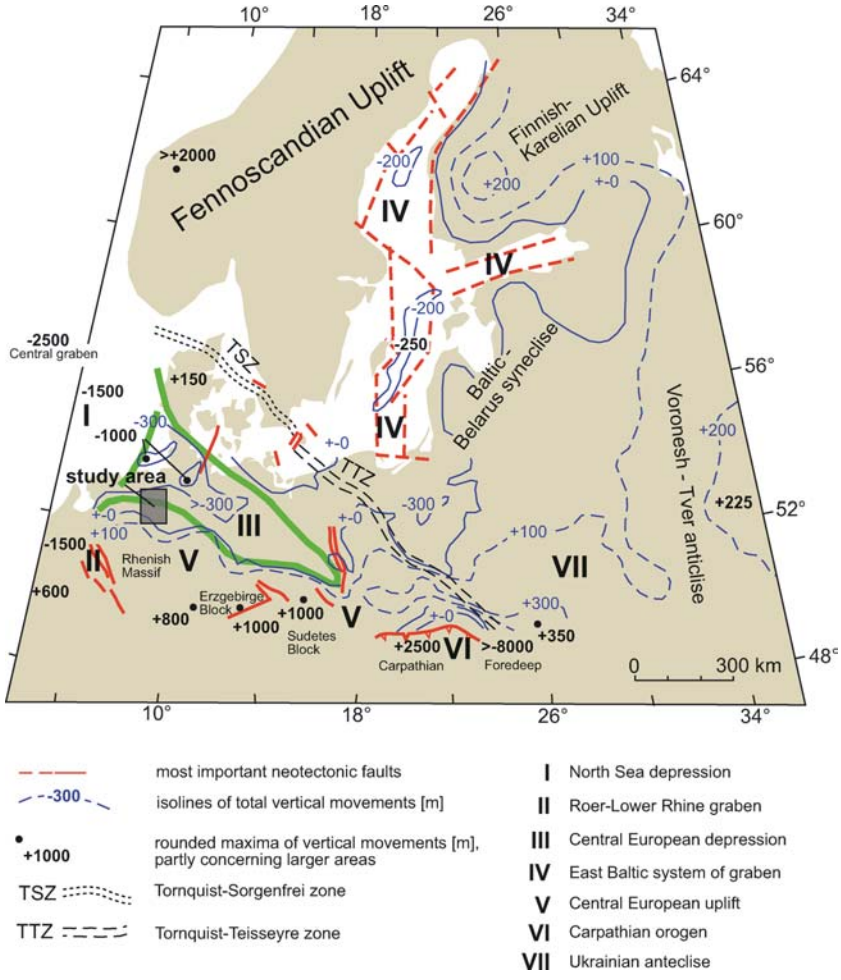

Fig. 17 Most important European areas of subsidence/uplift (*I–VII*) since the beginning of the Rupelian stage (~37 Ma ago) between 6–34° longitude and 48–64° latitude. The *green line* shows the position of the Central European depression. After Ludwig 2001a

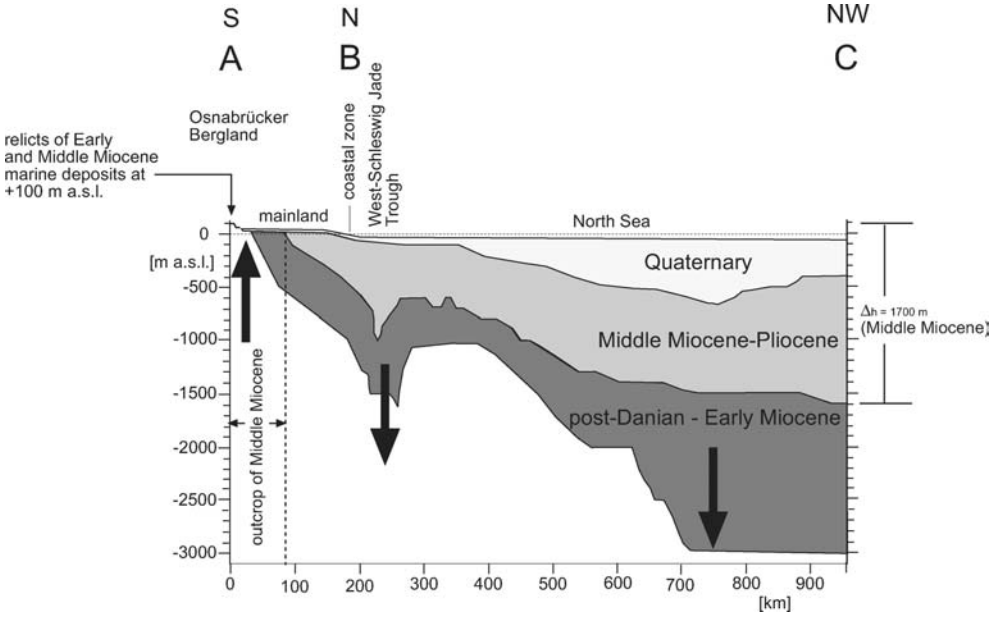

Fig. 18 Geological profile from A (Osnabrücker Bergland) over B (North Sea coast) to C (depocentre of Cenozoic sediments of the Central Graben). The depth of the Base Quaternary after Caston (1977), the depth of the Base Middle Miocene and the Base post-Danian after Kockel (1988). The geographical position of the profile is shown in Fig. 15

was established during the Pliocene (Bergerat 1987; Letouzey 1986; Müller et al. 1992) led to broad scale negative deflection of the lithosphere in the area of the North Sea Basin (Cloetingh and Kooi 1992) and to uplift of the Fennoscandian Shield (Ziegler 1990) and it is suggested by (Ziegler 1994) that the uplift of the

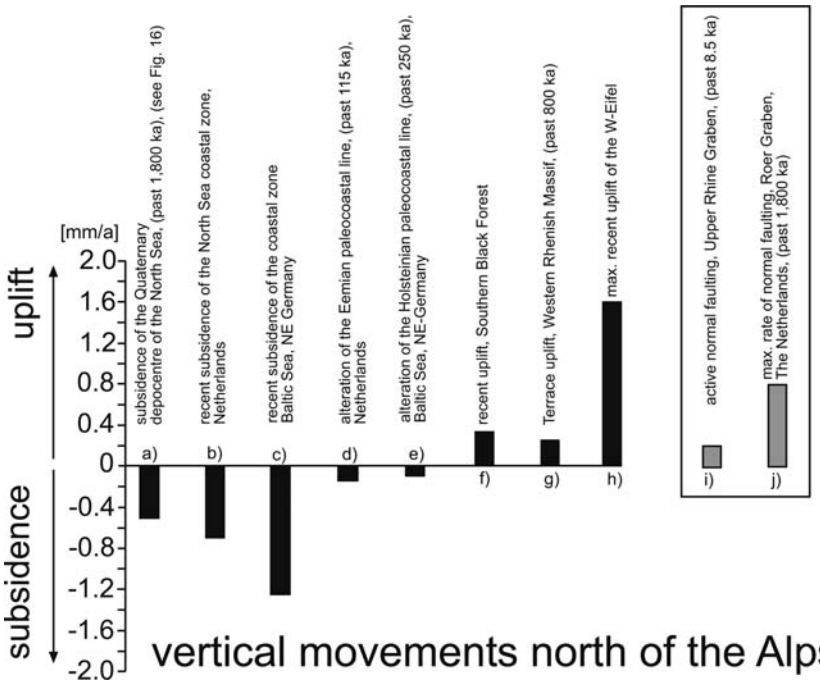

Fig. 19 Velocity rates of vertical movements (subsidence/uplift) north of the Alpine deformation front during the Quaternary, **a** subsidence rate of the North Sea Quaternary depocentre (−0.50 mm/a) during the past 1800 ka, database: (Caston 1977), (see Fig. 16); **b** recent subsidence rate of the North Sea coastal zone, the Netherlands, (−0.70 mm/a), determined from repeated precise levelling data, (after Kooi et al. 1998); **c** recent subsidence rate of the coastal zone, Baltic Sea, NE-Germany, (−1.25 mm/a), determined from repeated precise levelling data, (after Ihde et al. 1987); **d** post-Eemian subsidence rate of North Sea coastal-zone, the Netherlands, (−0.14 mm/a), determined from alterations of the Eemian paleocoastal line, (after Zagwijn 1983); **e** post-Holsteinian coastal subsidence rate of the Baltic Sea, NE Germany, (−0.10 mm/a), determined from alterations of the Holsteinian paleocoastal line, (after Ludwig and Schwab 1995); **f**recent maximum uplift rate of the Southern Black Forest [+0.33 mm/a], determined from repeated precise levelling data, (after Demoulin et al. 1998); **g** uplift of the Western Rhenish Massif at Cochem during the past 800 ka (+0.25 mm/a), determined from Terrace uplift, (after Meyer and Stets 1998); **h** maximum recent uplift rate of the West-Eifel (+1.60 mm/a), determined from repeated precise levelling data, (after Mälzer et al. 1983); **i** rate of active normal faulting in the Upper Rhein area (0.21 mm/a) during the past 8.5 ka, (after Meghraoui et al. 2001); **j** max. rate of active normal faulting in the Roer Valley Graben (0.80 mm/a) during the Quaternary (∼1.8 Ma), (after Geluk et al. 1994)

Massif Central, Vosges-Black Forest, Bohemian Massif and Rhenish shield is connected with the development of the modern stress field. Fig. 21 shows a geological profile (EF) through the southern part of the study area, after Geotectonic Atlas of NW-Germany (Baldschuhn et al. 2001).

The position of the profile is given in Fig. 4. The profile crosses the inversional anticline structures Rehden, Aldorf and Bockstedt, which show mostly gentle northward dipping overthrust faults. It is clearly visible that even the pre-Zechstein (brown), which can be found at a depth of between −5,000 and −2,000 m, was affected by the Upper Cretaceous inversional phase. A relatively thin Zechstein layer (salts) of between ∼100 and ∼500 m is evident in the southern part of the profile which becomes thicker in the northern part of the profile. This Zechstein layer separates the pre-Zechstein (brown) from the upper tectonic story (Lower + Middle Buntsandstein to Quaternary). It is mentioned by (Faccenna et al. 1995; Kossow et al. 2000; Nalpas et al. 1995; Poblet et al. 1997) that Zechstein salts can act as a detachment layer by a process of decoupling. The modern horizontal compressional stress field which is orientated in the study area with 150° (Fig. 1), is probably able to cause fault reactivation, flexural doming of the already present anticlinal structures or even tilting of the basin.

Conclusions

Active northward tilting of the NW-German Basin forces the River Hunte to flow in a northerly direction as shown by high linear correlation coefficient between the Base of Tertiary and the modern topography.

Plate tectonic processes (convergence of Africa–Eurasia, North Atlantic sea-floor spreading [ridge-push]) and crustal rebound (glacial unloading of the Weichselian ice cap) or ongoing basin subsidence have the potential to cause recent and subrecent crustal movements inside the NW-German Basin. Which of the processes (or a combination of them) causes the active movements remains to be discovered.

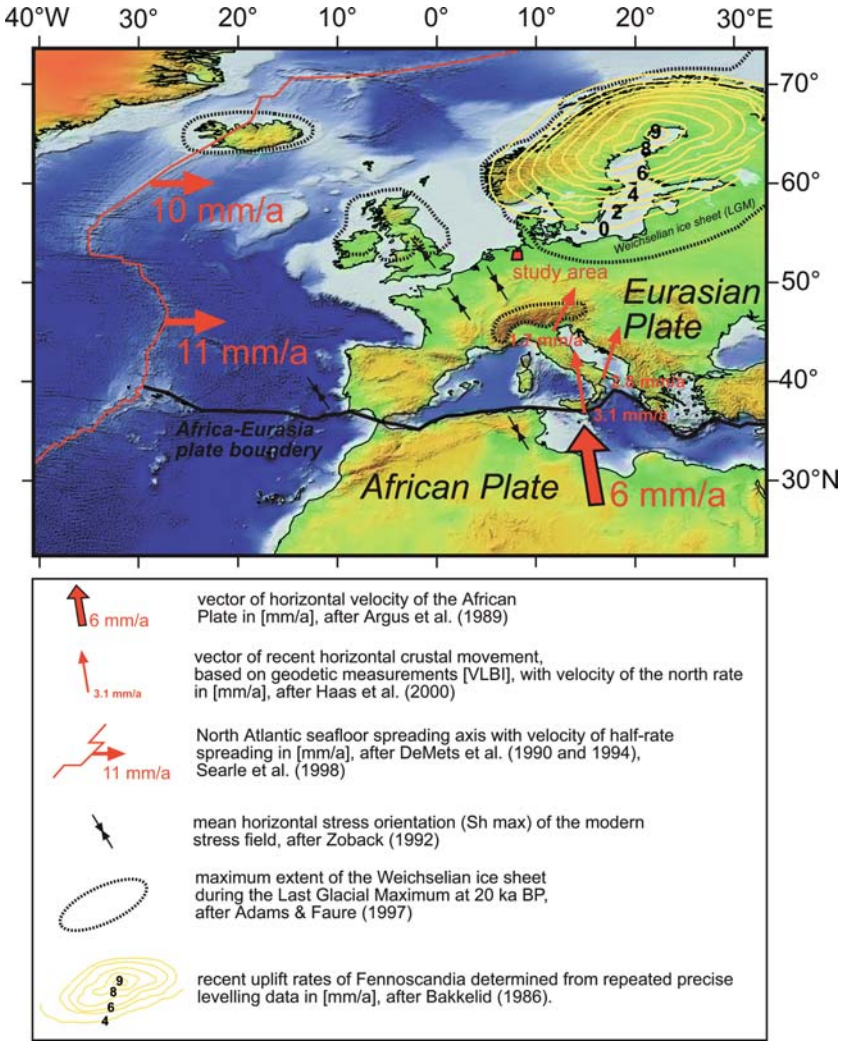

Fig. 20 Topographical and bathymetrical overview over northern Africa, Europe and the Atlantic ocean. The red motion vector shows the recent horizontal velocity of 6 mm/a of the African Plate relative to the Eurasian Plate (convergence) based on rotations around the Euler pole, (after Argus et al. 1989). The *red line* gives the position of the active Atlantic spreading ridge and transform faults with the total spreading rate of between 18–23 mm/a after the NUVEL-1A model (DeMets et al. 1990; DeMets et al. 1994; Searle et al. 1998). The *red arrows* give the recent horizontal crustal movement, based on geodetic measurements (VLBI), with velocity of the north rate in (mm/a), (after Haas et al. 2000). The *doubled black arrows* give the mean horizontal stress orientation (Sh max) of the modern stress field (after Zoback 1992). The *yellow isolines* show the recent uplift pattern of Fennoscandia of maximal 9 mm/a, derived from precise relevelling campaigns, (after Bakkelid 1986). The *dashed line* shows the maximum extend of the Weichselian ice sheet during the Last Glacial Maximum (LGM), (after Adams and Faure 1997). The position of the study area is given by the *red rectangle*

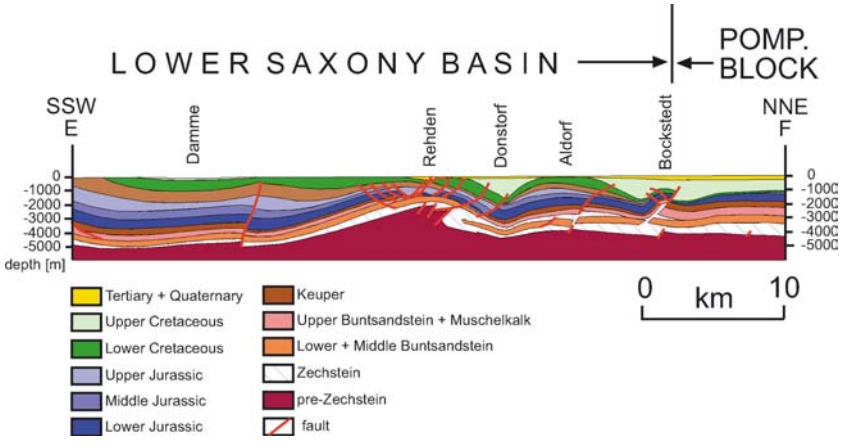

Fig. 21 Geological profile (EF), through a part of the NW-German Basin (Lower Saxony Basin, Pompeckj Block) from the pre-Zechstein (*brown*) to the Tertiary + Quaternary (*yellow*). The position of the profile is shown in Fig. 4. Faults are given in *red*, after Geotectonic Atlas of NW-Germany (Baldschuhn et al. 2001). Figure comes primary from Baldschuhn et al. 1991 and Binot et al. 1993

References

Adams JM, Faure H (1997) Preliminary vegetation maps of the world since the last glacial maximum: an aid to archaeological understanding. J Archaeol Sci 24:623–647

Anderson H-J, Indans J (1969) Fossilien aus dem Miocän vom "Tiefen Schafberger Stollen" bei Ibbenbühren/Westfalen. Fortschr Geol Rheinld u Westf 17:55–68

Anzidei M et al (2001) Insights into present-day crustal motion in the central Mediterranean area from GPS surveys. Geophy J Int 146:98–110

Argus DF, Gordon RG, DeMets C, Stein S (1989) Closure of the Africa-Eurasia-North America plate motion circuit and tectonics of the Gloria fault. J Geophys Res 94(B5):5585–5602
Bakkelid S (1986) The determination of rates of land uplift in Norway. Tectonophysics 130:307–326
Baldschuhn R, Frisch U, Kockel F (1985) Inversionsstrukturen in NW-Deutschland und ihre Genese. Z dt geol Ges 136:129–139
Baldschuhn R, Best G, Kockel F (1991) Inversion tectonics in the North-West German basin. In: Spencer AM (ed) Generation, accumulation, and production of Europeś hydrocarbons; III. Special Publication of the European Association of Petroleum Geoscientists, 1, pp 149–159
Baldschuhn R, Frisch U, Kockel F (1996) Geotektonischer Atlas von Nordwestdeutschland 1:300 000. BGR, Hannover
Baldschuhn R, Frisch U, Kockel F (1998) Der Salzkeil, ein strukturelles Requisit der saxonischen Tektonik. Z dt geol Ges 149(1):59–69
Baldschuhn R, Binot F, Fleig S, Frisch U, Kockel F (2001) Geotektonischer Atlas von Nordwest-Deutschland und dem deutschen Nordsee-Sektor - Strukturen, Strukturentwicklung, Paläogeographie -. Geol Jb A153:1–44. 3 CD-ROMs
Bankwitz P (1976) Rezente vertikale Erdkrustenbewegungen -Materialien zum tektonischen Bau von Europa-, scale 1:600.000. Zentralinstitut für Physik der Erde, Potsdam, Akademie der Wissenschaften der DDR, 47(Karte 8)
Bastos L, Osorio J, Barbeito A, Hein G (1998) Results from geodetic measurements in the western part of the African-Eurasian plate boundary. Tectonophysics 294:261–269
BEB (2002) Contour map of Base Tertiary, contour intervall of 25 m. BEB, unpublished 3D Seismic Data from the German Oil Industry, Hannover
Bergerat F (1987) Stress fields in the European platform at the time of Africa-Eurasia collision. Tectonics 6(2):99–132
Betz D, Führer F, Greiner G, Plein E (1987) Evolution of the lower Saxony Basin. Tectonophysics 137:127–170
BGR (1982) Geologische Übersichtskarten CC3110 + CC3910, 1:200 000. Bundesanstalt für Geowissenschaften und Rohstoffe (BGR), Hannover
Binot F, Gerling P, Hiltmann W, Kockel F, Wehner H (1993) The petroleum system in the lower Saxony Basin. In: Spencer AM (ed) Generation, accumulation, and production of Europeś hydrocarbons. Special Publication of the European Association of Petroleum Geoscientists, 3, pp 121–139
Bird P, Gratz AJ (1990) A theory for buckling of the mantle lithosphere and Moho during compressive detachments in continents. Tectonophysics 177:325–336
Boigk H (1968) Gedanken zur Entwicklung des Niedersächsischen Tektogens. Geol Jb 85:861–900
Boigk H (1981) Erdöl und Erdgas in der Bundesrepublik Deutschland. Ferdinant Enke Verlag, Stuttgart, p 330
Böse (1995) Problems Of Dead Ice And Ground Ice In The Central Part Of The North European Plain. Quaternary Int 28:123–125
Brown LD, Reilinger RE (1986) Epirogenic and intraplate movements, active tectonics—studies in geophysics. National Academy Press, Washington, pp 30–45
Burov EB, Lobkovsky LI, Cloething S, Nikishin AM (1993) Continental folding in Central Asia (Part II): constraints from geological observations. Tectonophysics 226:73–87
Camelbeeck T, Meghraoui M (1996) Large earthquakes in northern Europe more likely than once thought. Eos 77(42):405–409
Campell J, Nothnagel A (2000) European VLBI for crustal dynamics. J Geodynamics 30:321–326
Caspers G et al (1995) Niedersachsen. In: Benda L (ed) Das Quartär Deutschlands. Gebrüder Borntraeger, Stuttgart, pp 23–58
Caspers G, Freund H (2001) Vegetation and climate in the Early- and Pleni-Weichselian in northern central Europe. J Quaternary Sci 16(1):31–48
Caston VND (1977) A new isopachyte map of the Quaternary of the North Sea, quaternary deposits of the Central North Sea. 1. Report—Institute of Geological Sciences, United Kingdom, pp 1–8
Cloetingh S, Kooi H (1992) Intraplate stresses and dynamical aspects of rifted basins. Tectonophysics 215:167–185
Cloetingh S, Gradstein FM, Kooi H, Grant AC, Kaminski M (1990) Plate reorganization: a cause of rapid late Neogene subsidence and sedimentation around the North Atlantic? J Geol Soc Lond 147:495–506
Cloetingh S, Sassi W, Horvath F (1993) The origin of sedimentary basins: state of the art and first results of the task force. Tectonophysics 225:7–10
Cloetingh S, Eldholm O, Larsen BT, Gabrielsen RH, Sassi W (1994) Dynamics and extensional basin formation and inversion: introduction. Tectonophysics 240:1–9
Cloetingh S, Argenio BD, Catalano R, Horvath F, Sassi W (1995) Interplay of extension and compression in basin formation: introduction. Tectonophysics 252:1–5
Cloetingh S, Ben-Avraham Z, Sassi W, Horvath F (1996) Dynamics of basin formation and strike-slip tectonics. Tectonophysics 266:1–10
Cloetingh S, Fernandez M, Munoz JA, Sassi W, Horvath F (1997) Structural controls on sedimentary basin evolution: introduction. Tectonophysics 282:11–18
DeMets C, Gordon RG, Argus DF, Stein S (1990) Current plate motions. Geophys J Int 101:425–478
DeMets C, Gordon RG, Argus DF, Stein S (1994) Effect of recent revision to the geomagnetic reversal time scale on estimates of current plate motions. Geophys Res Lett 21(20):2191–2194
Demoulin A, Launoy T, Zippelt K (1998) Recent crustal movements in the southern Black Forest (western Germany). Geol Rundsch 87:43–52
Devoti R et al (2002) Geodetic control on recent tectonic movements in the central Mediterranean area. Tectonophysics 346:151–167
DGK-Arbeitskreis (1979) On the ''map of height changes in the Federal Republic of Germany—status 1979'' 1:1000 000. Allg Vermessungsnachr 86:362–363
Dulce J-C, Gronemeier K (1982) Linearanalysen auf Satelliten- und Luftbildern in verschiedenen geologischen Einheiten - Anwendbarkeit in der Hydrogeologie. Z dt geol Ges 133:535–549
Faccenna C, Nalpas T, Brun J-B, Davy P (1995) The influence of pre-existing thrust faults on normal fault geometry in nature and in experiments. J Struct Geol 17(8):1139–1149
Ferhat G, Feigl KL, Ritz J-F, Souriau A (1998) Geodetic measurement of tectonic deformation in the southern Alps and Provence, France, 1947–1994. Earth Planet Sci Lett 159:35–46
Frischbutter A (2001) Recent vertical movements (map 4) (Neogeodynamica Baltica IGCP-Project 346). Brandenburgische Geowiss Beitr 8(1):27–31
Geluk MC et al (1994) Stratigraphy and tectonics of the Roer Valley Graben. Geologie en Mijnbouw 73:129–141
Gölke M, Coblentz D (1996) Origins of the European regional stress field. Tectonophysics 266:11–24
Gramann F (1966) Das Oligozän der Hessischen Senke als Bindeglied zwischen Nordseebecken und Rheintalgraben. Z deutsch geol Ges 115:497–514
Gramann F, Kockel F (1988) Palaeogeographical, lithological, palaeoecological and palaeoclimatic development of the Northwest European Tertiary Basin. In: Vinken R (ed) The Northwest European Tertiary Basin (Results of the International Geological Correlation Programme Project No 124). Geol Jb A100:428–441
Grollimund B, Zoback MD (2000) Post glacial lithospheric flexure and induced stresses and pore pressure changes in the northern North Sea. Tectonophysics 327:61–81
Grünthal G, Stromeyer D (1992) The Recent Crustal Stress Field in Central Europe: Trajectories and Finite Element Modeling. J Geophys Res 97(B8):11805–11820
Grünthal G, Stromeyer D (2001) Direction of recent maximal stress and epicenter map of tectonic earthquakes (maps 5 and 6). Neogeodynamica Baltica IGCP-Project 346. Brandenburgische Geowiss Beitr 8(1):33–37

Gudmundsson A (1999) Postglacial crustal doming, stresses and fracture formation with application to Norway. Tectonophysics 307:407–419

Haack W (1932) Über das marine Mittelmiozän von Lechtingen bei Osnabrück und die Umwandlung des Keupermergels in seinem Liegenden. Jahrbuch der Preußischen Geologischen Landesanstalt zu Berlin 53:553–576

Haas R, Guguen E, Scherneck H-G, Nothnagel A, Campell J (2000) Crustal motion results derived from observations in the European geodetic VLBI network. Earth Planets Space 52:759–764

Harrison RW, Hoffman D, Vaughn JD, Palmer JR (1999) An example of neotectonism in a continental interior—Thebes Gap, Midcontinent, United States. Tectonophysics 305:399–417

Hiltermann H (1984) Tertiär. In: Klassen H (ed), Geologie des Osnabrücker Berglandes. Naturwissenschaftliches Museum Osnabrück, Osnabrück, pp 463–497

Hinsch W (1988) Section M-M': the Federal Republic of Germany, Lübeck (SE)-Schnelsen-Eiderstedt-Pellworm (NW) (based on borehole data with seismic control) (Results of the International Geological Correlation Programme Project No 124). Geol Jb A100:127–128

Hinsch W, Ortlam D (1974) Stand und Probleme der Gliederung des Tertiärs in Nordwestdeutschland. Geol Jb A16:3–25

Hinsch W, Kaever M, Martini E (1978) Die Fossilführung des Erdfalls von Nieheim (SE-Westfalen) und seine Bedeutung für die Paläogeographie im Campan und Miozän. Paläont Z 52(3/4):219–245

Hinze C (1979) Erläuterungen zu Blatt Nr. 3614 Wallenhorst - Geologische Karte von Niedersachsen 1 : 25000- Niedersächsisches Landesamt für Bodenforschung, Hannover, p 154

Houtgast RF, van Balen RT (2000) Neotectonics of the Roer Valley Rift System, the Netherlands. Glob Planet Change 27:131–146

Houtgast RF, Van Balen RT, Bouwer LM, Brand GBM, Brijker JM (2002) Late Quaternary activity of the Feldbiss Fault Zone, Roer Valley Rift System, the Netherlands, based on displaced fluvial terraces. Tectonophysics 352:295–315

Huisink M (1998) Changing river styles in response to climate change. Examples from the Maas and Vecht during the Weichselian Pleni- and Lateglacial, Vrije Universteit Amsterdam, Wageningen, p 127

Ihde J, Steinberg J, Ellenberg J, Bankwitz E (1987) On recent vertical crustal movements derived from relevellings within the terretory of the GDR. Gerlands Beitr Geophysik 96:206–217

James TS, Lambert A (1993) A comparison Of VLBI data with the Ice-3G glacial rebound model. Geophys Res Lett 20(9):871–874

Jaritz W (1973) Zur Entstehung der Salzstrukturen Nordwestdeutschlands. Geol Jb A10:3–77

Jaritz W (1980) Einige Aspekte der Entwicklungsgeschichte der nordwestdeutschen Salzstöcke. Z dt geol Ges 131:387–408

Jaritz W (1992) Fortschritte und offene Fragen zur Entstehung der Salzstrukturen NW-Deutschlands. Nds Akad Geowiss Veröfftl 8:16–24

Johnston P, Wu P, Lambeck K (1998) Dependence of horizontal stress magnitude on load dimension in glacial rebound models. Geophys J Int 132:41–60

Kahle H-G et al (1998) The strain rate field in the eastern Mediterranean region, estimated by repeated GPS measurements. Tectonophysics 294:237–252

Kaltwang J (1992) Die pleistozäne Vereisungsgrenze im südlichen Niedersachsen und im östlichen Westfalen. Mitt geol Inst Univ Hannover 33:1–161

Klemann V, Wolf D (1998) Modelling of stresses in the Fennoscandian lithosphere induced by Pleistocene glacations. Tectonophysics 294:291–303

Kockel F (1988) The paleogeographic maps, the northwest European Tertiary Basin (Results of the International Geological Correlation Programme Project No 124). Geol Jb A100:428–441

Kooi H, Cloetingh S (1989) Some consequences of compressional tectonics for extensional models of basin subsidence. Geologische Rundschau 78(1):183–195

Kooi H, Cloetingh S, Remmelts G (1989) Intraplate stresses and the stratigraphic evolution of the North Sea Central Graben. Geologie en Mijnbouw 68:49–72

Kooi H, Hettema M, Cloetingh S (1991) Lithospheric dynamics and the rapid Pliocene-Quaternary susidence phase in the southern North Sea Basin. Tectonophysics 192:245–259

Kooi H, Johnston P, Lambeck K, Smither C, Molendijk R (1998) Geological causes of recent (~100 yr) vertical land movement in the Netherland. Tectonophysics 299:297–316

Kossow D, Krawczyk C, McCann T, Strecker M, Negendank JFW (2000) Style and evolution of salt pillows and related structures in the northern part of the Northeast German Basin. Int J Earth Sci 89:652–664

Kronberg P (1991) Crustal fracturing and intraplate tectonics in the area between the North Sea and the Alps: a comparison of Landsat-derived fractures with existing map data. Tectonophysics 195:261–269

Krull P, Wegner T (1988) Einsatz der Fernerkundung in der Kohlenwasserstoff-Forschung im Nordteil der DDR. Zeitschrift für angewandte Geologie 34(8):235–239

Krull P, Langer M, Trembich G, Wegner T (1985) Methodische Beiträge zur Interpretation von Fernerkundungsdaten im Nordteil der DDR. Zeitschrift für angewandte Geologie 31(12):295–300

Kuster H, Meyer K-D (1979) Glaziäre Rinnen im mittleren und nordöstlichen Niedersachsen. Eiszeitalter und Gegenwart 29:135–156

Lagerbäck R (1990) Late Quaternary faulting and paleoseismicity in northern Fennoscandia, with particular reference to the Lansjärv area, northern Sweden. Geologiska Föreningens i Stockholm Förhandlingar 112(4):333–354

Leonhard T (1988) Zur Berechnung von Höhenänderungen in Norddeutschland -Modelldiskussion, Lösbarkeitsanalyse und numerische Ergebnisse-. Doctoral thesis, Universität Hannover, p 158

Letouzey J (1986) Cenozoic paleo-stress pattern in the Alpine Foreland and structural interpretation in a platform basin. Tectonophysics 132:215–231

Leydecker G et al (1980) Das Beben vom 2. Juni 1977 in der norddeutschen Tiefebene bei Soltau. Geol Jb E18:3–18

Leydecker G (2002a) Das Erdbeben vom 11. Juli 2002 in Weyhe südlich Bremen im Norddeutschen Tiefland. Bundesanstalt für Geowissenschaften und Rohstoffe (BGR), Tagebuch Nr. 12 106/02, 1–6

Leydecker G (2002b) Erdbebenkatalog für die Bundesrepublik Deutschland mit Randgebieten für die Jahre 800–2001. Bundesanstalt für Geowissenschaften und Rohstoffe (BGR). - Datenfile http://www.bgr.de/quakecat.

Leydecker G, Kopera JR (1999) Seismological hazard assessment for a site in Northern Germany, an area of low seismicity. Eng Geol 52:293–304

LGN (1898) Preussische Landesaufnahme 1:25000. LGN -Landesvermessung + Geobasisinformation Niedersachsen-, Hannover

LGN (1994) Topografische Karte 1:25000. LGN -Landesvermessung + Geobasisinformation Niedersachsen-, Hannover

Liedtke H (1981) Die nordischen Vereisungen in Mitteleuropa. Forschungen zur Deutschen Landeskunde, Trier, p 307

Ludwig AO (2001a) Vertical movements since the beginning of Rupelian stage (map 1). Neogeodynamica Baltica IGCP-Project 346. Brandenburgische Geowiss Beitr 8(1):5–12

Ludwig AO (2001b) Recent position of surfaces of Holsteinian interglacial marine and limnic sediments, and of Saalian glacial river terraces. Neogeodynamica Baltica IGCP-Project 346. Brandenburgische Geowiss Beitr 8(1):21–25

Ludwig AO, Schwab G (1995) Neogeodynamica Baltica - ein internationales Kartenprojekt (IGCP-Projekt Nr. 346). Deutsche Beiträge zur Charakterisierung der vertikalen Bewegungen seit Beginn des Rupelian (Unteroligozän) bzw. seit Ende der Holstein-Zeit. Brandenburgische Geowiss Beitr 2(2):47–57

Maddy D, Bridgland DR, Green CP (2000) Crustal uplift in southern England: evidence from the river terrace records. Geomorphology 33:167–181

Mälzer H, Hein G, Zippelt K (1983) Height changes in the Rhenish Massif: determination and analysis. In: Fuchs K, von Gehlen K, Mälzer H, Murawski H, Semmel A (eds) Plateau uplift—the Rhenish shield—a case history. Springer, Berlin Heidelberg New York, pp 164–177

Marshak S, Van der Pluijm BA, Hamburger M (1999) Preface—the tectonics of continental interiors. Tectonophysics 305:7–10

Meghraoui M et al (2001) Active normal faulting in the upper Rhine Graben and Paleoseismic identification of the 1356 Basel earthquake. Science 293:2070–2073

Meier T (1996) Früh- und spätweichselzeitliche Flugsand- und Sandlößvorkommen im Huntetal (Niedersachsen). Diploma Thesis, Universität Kiel, p 58

Meyer W, Stets J (1998) Junge Tektonik im Rheinischen Schiefergebirge und ihre Quantifizierung. Z dt geol Ges 149(3):359–379

Milne GA et al (2001) Space-geodetic constraints on glacial isostatic adjustment in Fennoscandia. Science 291:2381–2385

Minister JB (1978) Present-day plate motions. J Geophys Res 83(B11):5331–5354

Mitrovica JX, Davis JL, Shapiro II (1994) A spectral formalism for computing three-dimensional deformations due to surface loads 2. Present-day glacial isostatic adjustment. J Geophys Res 99(B4):7075–7101

Mol J, Vandenberghe J, Kasse C (2000) River response to variations of periglacial climate in mid-latitude Europe. Geomorphology 33:131–148

Müller B et al (1992) Regional patterns of tectonic stress in Europe. J Geophys Res 97(B8):11783–11803

Müller B, Reinecker J, Heidbach O, Fuchs K (2000) The 2000 release of the World Stress Map. Available online at http://www.world-stress-map.org. Cited on 1 October 2001

Nalpas T, Le Douaran S, Brun J-P, Unternehr P, Richert J-P (1995) Inversion of the Broad Fourteens Basin (offshore Netherlands), a small-scale model inverstigation. Sediment Geol 95:237–250

Nelson WJ, Denny FBD, Follmer LR, Masters JM (1999) Quaternary grabens in southernmost Illinois: deformation near an active intraplate seismic zone. Tectonophysics 305:381–397

Ness D (1994) Gewässerkundliche Beschreibung der Hunte. In: Ackermann R (ed) Die Hunte -Porträt eines nordwestdeutschen Flusses-. Isensee Verlag, Oldenburg, pp 27–42

Nikishin AM, Cloething S, Lobkovsky LI, Burov EB, Lankreijer AC (1993) Continental folding in Central Asia (Part I): constraints from geological observations. Tectonophysics 226:59–72

NLfB (1993) Quartärgeologische Übersichtskarte von Niedersachsen und Bremen 1:500.000. Niedersächsisches Landesamt für Bodenforschung (NLfB), Hannover

Ortlam D, Vierhuff H (1978) Aspekte zur Geologie des höheren Känozoikums zwischen Elbe und Weser-Aller. N Jb Geol Paläont Mh 7:408–426

Poblet J, McClay K, Storti F, Munoz JA (1997) Geometries of syntectonic sediments associated with single-layer detachment folds. J Struct Geol 19(3–4):369–381

Pyritz E (1972) Binnendünen und Flugsandebenen im Niedersächsischen Tiefland. Göttinger Geographische Abhandlungen 61:1–153

Reilinger RE, McClusky SC, Oral MB, King RW, Toksoz MN (1997) Global positioning system measurements of present-day crustal movements in the Arabian-Africa-Eurasia plate collision zone. J Geophys Res 102(B5):9983–9999

Richardson RM (1992) Ridge forces, absolute motions, and the intraplate stress field. J Geophys Res 97(B8):11739–11748

Schwab G (1981) Paläotektonische, neotektonische und rezente Krustenbewegung in Gebiet der DDR. Z geol Wiss 9(11):1223–1236

Schwab G (1996) Zum Relief der Quartärbasis in Norddeutschland. Bemerkungen zu einer neuen Karte. Z geol Wiss 24:343–349

Schwab G, Tetschke H-J, Jubitz KH (1973) Zur Raum-Zeit-Beziehung zwischen rezenten Krustenbewegungen und Paläotektonik im Breich der Norddeutsch-Polnischen Senke. Zeitschrift für angewandte Geologie 19(11):579–586

Schwan J (1988) The structure and genesis of Weichselian to early Holocene Aeolian Sand sheets in western Europe. Sediment Geol 55:197–232

Sclater JG, Christie PAF (1980) Continental stretching of the Post-Mid-Cretaceous subsidence of the Central North Sea. J Geophys Res 85(B7):3711–3739

Searle RC et al (1998) The Reykjanes Ridge: structure and tectonics of a hot-spot-influenced, slow-spreading ridge, from multibeam bathymetry, gravity and magnetic investigations. Earth Planet Sci Lett 160:463–478

Sesören A (1976) Lineament analyses from ERTS (Landsat) images of the Netherlands. Geologie En Mijnbouw 55(1–2):61–67

Sharma PV (1984) The Fennoscandian uplift and glacial isostasy. Tectonophysics 105:249–262

Sirocko F, Szeder T, Seelos C, Lehne R, Rein B, Schneider WM, Dimke M (2002) Young tectonic and halokinetic movements in the North-German-Basin: iśś effect on formation of rivers and surface morphology. Neth J Geosci/Geologie en Mijnbouw 81(3–4):431–441

Stackebrandt W, Garetzky R, Aizberg R, Karabanov A, Ludwig AO, Ostaficzuk S (2001) The neogeodynamics of northern central Europe (Results of IGCP-Project No 346):''Neogeodynamica Baltica''. Z geol Wiss 29(1/2):13–16

Steward IS, Sauber J, Rose J (2000) Glacio-seismotectonics: ice sheets, crustal deformation and seismicity. Quaternary Sci Rev 19:1367–1389

Streif HJ (1991) Zum Ausmaß und Ablauf eustatischer Meeresspiegelschwankungen im südlichen Nordseegebiet seit Beginn des Letzten Interglazials. In: Frenzel B (ed) Klimageschichte der letzten 130 000 Jahre. Gustav Fischer Verlag, Stuttgart, New York pp 231–249

Sue C et al (2000) Active deformation in the inner western Alps inferred from comparison between 1972-classical and 1996-GPS geodetic surveys. Tectonophysics 320:17–29

Talwani P (1999) Fault geometry and earthquakes in continental interiors. Tectonophysics 305:371–379

Thiermann A (1970) Erläuterungen zu Blatt 3712 -Geologische Karte von Nordrhein-Westfalen 1:25 000-. Geologisches Landesamt Nordrhein-Westfalen, Krefeld, p 243

Thorne JA, Watts AB (1989) Quantitative analyses of North Sea Subsidence. Am Assoc Petrol Geol Bull 73(1):88–116

USGS (2002) Earthquake Hazards Program -National Earthquake Information Center, World Data Center for Seismology, Denver. http://www.neic.usgs.gov. Cited on 1 February 2002

Vaikmäe R, Böse M, Michel FA, Moormann BJ (1995) Changes in permafrost conditions. Quaternary Int 28:113–118

Vandenberghe J (1992a) Geomorphology and climate of the cool oxygen isotope stage 3 in comparison with the cold stages 2 and 4 in the Netherlands. Z Geomorph N F 86:65–75

Vandenberghe J (1993) Changing fluvial processes under changing periglacial conditions. Zeitschrift für Geomorphologie 88:17–28

Vandenberghe J (1995a) The role of rivers in palaeoclimate reconstruction. In: Frenzel B (ed) European river activity and climate change during the Lateglacial and Early Holocene. Gustav Fischer Verlag, Stuttgart, Jena, New York, pp 11–19

Vandenberghe J (1995b) Timescale, Climate And River Development. Quaternary Sci Rev 14:631–638

Vandenberghe J, Pissart A (1993) Permafrost changes in Europe during the last glacial. Perm Periglac Processes 4:121–135

Vandenberghe J, Kasse C, Bohncke S, Korzarski S (1994) Climate-related river activity at the Weichselian-Holocene transition: a comparative study of the Warta and Maas rivers. Terra Nova 6:476–485

Vanneste K, Meghraoui M, Camelbeek T (1999) Late Quaternary earthquake-related soft-sediment deformation along the Belgian portion of the Feldbiss Fault, Lower Rhine Graben system. Tectonophysics 309:57–79

Vierhuff H (1967) Untersuchungen zur Stratigraphie und Genese der Sandlössvorkommen in Niedersachsen. Mittteilungen aus dem Geologischen Institut der Technischen Hochschule Hannover 5:1–99

Wahlström R (1993) Fennoscandian seismicity and its relation to the isostatic rebound. Glob Planet Change 8:107–112
van Wees JD, Cloetingh S (1996) 3D Flexure and intraplate compression in the North Sea Basin. Tectonophysics 266:343–359
Wolf D (1986) Glacio-isostatic adjustment in Fennoscandia revisited. J Geophysics 59:42–48
Wolf D (1987) An upper bound on lithosphere thickness from glacio-isostatic adjustment in Fennoscandia. J Geophysics 61:141–149
Wolf D (1993) The changing role of the lithosphere in models of glacial isostasy: a historical review. Glob Planet Change 8:95–106
Wolf D (1996) Note on estimates of the glacial-isostatic decay spectrum for Fennoscandia. Geophys J Int 127:801–805
Wu P, Johnston P, Lambeck K (1999) Postglacial rebound and fault instability in Fennoscandia. Geophs J Int 139:657–670
Wübbelmann H (1993) Vergleich zwischen Höhen im DHHN 85 und im Nivellementnetz 1960. Die Wiederhohlungsmessungen 1980 bis 1985 im Deutschen Haupthöhennetz und das Haupthöhennetz 1985 der Bundesrepublik Deutschland. Arbeitsgemeinschaft der Vermessungsverwaltungen der Länder der Bundesrepublik (ADV) - Arbeitskreis Höhenfestpunktfeld und Schwerefestpunktfeld (AK Niv), Bayrisches Landesvermessungsamt, München, pp 155–165
Zagwijn WH (1983) Sea-level changes in the Netherland during the Eemian. Geologie en Mijnbouw 62:437–450
Zagwijn WH (1989) The Netherlands during the Tertiary and the Quaternary: a case history of Coastal Lowland evolution. Geologie en Mijnbouw 68:107–120
Ziegler PA (1990) Geological Atlas of western and central Europe, 2nd edn. Shell Internationale Petroleum Maatschappij B.V. and Geol. Soc. London, Elsevier, Amsterdam, p 239
Ziegler PA (1994) Cenozoic rift systems of western and central Europe: an overview. Geologie en Mijnbouw 73:99–127
Ziegler P, Cloetingh S, van Wees J-D (1995) Dynamics of intraplate compressional deformation: the Alpine foreland and other examples. Tectonophysics 252:7–59
Zoback ML (1992) First- and second-order patterns of stress in the lithosphere: the world stress map project. J Geophys Res 97(B8):11703–11728
Zoback MD et al (1993) Stresses in the lithosphere and sedimentary basin formation. Tectonophysics 226:1–13
Zoback MD, Grollimund B (2001) Impact of deglaciation on present-day intraplate seismicity in eastern North America and western Europe. Earth Planet Sci 333:23–33
Zoback ML, Zoback MD, Adams J, Assumpca M, Bell S (1989) Global patterns of tectonic stress. Nature 341:291–298